in LDLT or liver cirrhosis. We therefore investigated the effect of loss of liver volume or development of cirrhosis on the serum levels of recombinant human HGF. When recombinant human HGF (0.1 mg/kg) was injected intravenously into rats with 70% partial hepatectomy, the serum levels of human HGF increased to 341.2 ± 55.1 ng/ml at 5 min (Fig. 1A). A significant increase in serum HGF levels was also observed at 10, 30 and 120 min, and the half-life was prolonged (in comparison to normal rats) to 3.8 min. Similarly, the bolus injection of recombinant human HGF into rats with liver cirrhosis led to significantly elevated levels of serum human HGF at each time point and a prolonged half-life (4.4 min).

Conversely, when recombinant human HGF (0.1 mg/kg) was injected to portal veins in normal rats, the serum level of human HGF was only 17.8 ± 5.94 ng/ml 5 min after the injection (Fig. 1B). This is lower than after the intravenous injection; furthermore, the recombinant human HGF injected via portal vein was rapidly decreased with a half-life of 3.0 min (Fig. 1B). In comparison with normal rats, those with 70% partial hepatectomy exhibited significantly higher

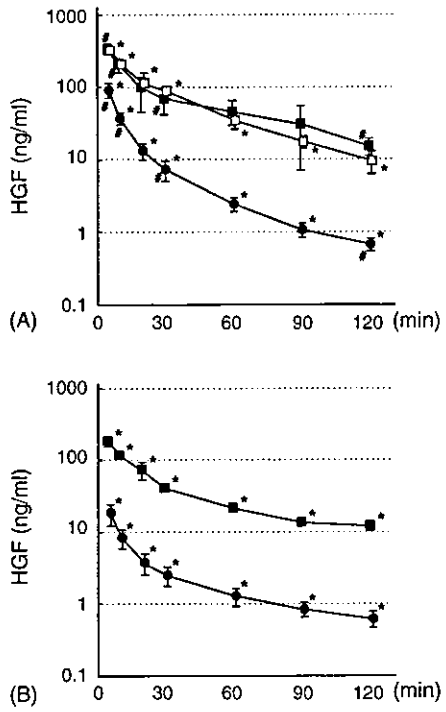

Fig. 1. Serum levels of recombinant human HGF following bolus injection in normal, hepatectomized, and cirrhotic rats. (A) Recombinant human HGF (0.1 mg/kg) was administered intravenously to normal (●: $n = 4$), partially hepatectomized (■: : $n = 3$–4), and cirrhotic (□: $n = 4$) rats, and serum human HGF was determined 5, 10, 20, 30, 60, 90 and 120 min by ELISA as described in Section 2. The serum levels of human HGF at 5 min and its half-life were 89.7 ± 20.6 ng/ml and 2.4 min in normal rats, 341.2 ± 55.1 ng/ml and 3.8 min in rats with partial hepatectomy, and 319.8 ± 22.3 ng/ml and 4.4 min in rats with CDAA diet-induced liver cirrhosis. * and #, $P < 0.05$. (B) Recombinant human HGF was injected via the portal vein in normal (●: $n = 4$) and partially hepatectomized (■: : $n = 3$–4) rats. The serum level of human HGF at 5 min and its half-life were 17.8 ± 5.9 ng/ml and 3.0 min in normal rats and 180.5 ± 29.6 ng/ml and 5.3 min in rats with partial hepatectomy. *, $P < 0.05$.

(180.5 ± 29.6 ng/ml at 5 min) levels of serum HGF following portal vein injection of the recombinant protein, and the recombinant protein had a prolonged half-life (5.3 min). These results suggest that the clearance of recombinant human HGF is dependent on liver volume or the number of hepatocytes, and suggest that the recombinant human HGF is trapped primarily in the liver.

3.2. Tissue distribution of recombinant human HGF administered intravenously or via portal vein

To address whether the liver is the primary organ targeted by recombinant human HGF, we examined tissue distribution of recombinant human HGF administered intravenously or via portal vein. Various tissue samples were obtained 5 min after the bolus injection of recombinant human HGF, and the HGF content of the tissues was measured by ELISA. When recombinant human HGF was administered intravenously, the liver, spleen, adrenal gland, and kidneys contained large amounts of human HGF (290.2 ± 38.3, 582.2 ± 205.0, 278.1 ± 114.1 and 101.3 ± 19.3 ng/g wet tissue, respectively) (Fig. 2, open columns). There were small amounts of human HGF in the lungs, pancreas, and large intestine (16.2 ± 3.2, 6.2 ± 0.9, and 2.0 ± 0.2 ng/g wet tissue, respectively). Although the HGF level per tissue weight in spleen was higher than that in liver, we consider human HGF administered intravenously to be primarily distributed to the liver because the weight of the liver is approximately 20-fold larger than that of the spleen. In contrast, when recombinant human HGF was injected via the portal vein, HGF content in the liver tissues increased to 519.5 ± 218.0 ng/g wet tissue (Fig. 2, closed columns). In comparison with intravenous injection, human HGF levels in extra-hepatic organs, including spleen, adrenal gland, kidney, and lungs, were significantly reduced. These results indicate that the liver is the organ predominantly targeted by intravenously administered recombinant human HGF, and the possibility that portal vein injection of the recombinant protein reduces the effects of HGF on extra-hepatic organs.

3.3. Intravenously injected recombinant human HGF effectively induces c-Met tyrosine phosphorylation

Recombinant human HGF, intravenously administered in a bolus, disappeared from serum with a short half-life. Therefore, we investigated whether a single bolus injection of recombinant human HGF induced tyrosine phosphorylation of c-Met, a specific receptor for HGF, in liver tissues (Fig. 3). Various amounts of recombinant human HGF (0.03, 0.1, 0.3 and 1.0 mg/kg) were injected intravenously in less than 10 s. When 0.1 mg/kg or greater recombinant HGF was administered, c-Met tyrosine phosphorylation was induced 30 min after the injection, and expression of c-Met decreased in parallel with the dose of recombinant HGF. Tyrosine phosphorylation of c-Met was close to background in rats given 0.03 mg/kg of recombinant HGF.

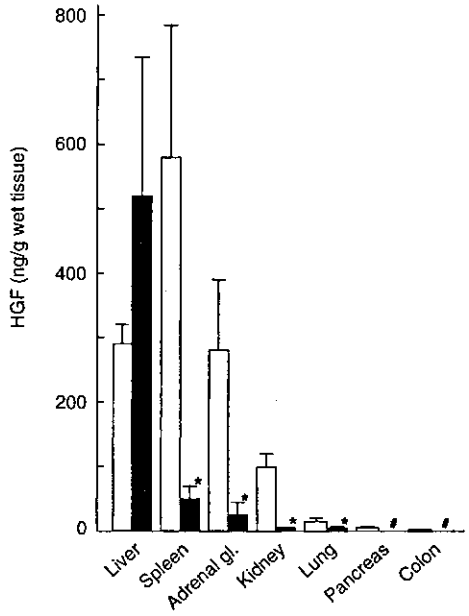

Fig. 2. Tissue distribution of recombinant human HGF administered intravenously or via the portal vein. Various tissue samples were obtained 5 min after bolus injection of recombinant human HGF (0.1 mg/kg). Tissue extracts were prepared and human HGF contents were measured by ELISA as described in Section 2. When recombinant human HGF was injected intravenously, a large amount of human HGF was observed in the liver, spleen, adrenal gland, and kidney (290.2 ± 38.3, 582.2 ± 205.0, 278.1 ± 114.1 and 101.3 ± 19.3 ng/g wet tissue, respectively). The amount was smaller in lung, pancreas, and large intestine (16.2 ± 3.2, 6.2 ± 0.9 and 2.0 ± 0.2 ng/g wet tissue, respectively) (open columns) ($n = 4$). Bolus injection via portal vein significantly reduced the distribution of this protein to extra-hepatic organs (spleen, adrenal gland, kidney, and lung), while HGF content in liver tissues was increased to 519.5 ± 218.0 ng/g wet tissue (closed columns) ($n = 4$). #, HGF content in pancreas and large intestine of rats that received human HGF via the portal vein were not determined. *, $P < 0.05$ in comparison with HGF content in each organ of rats treated intravenously with recombinant human HGF.

3.4. Rats with partial hepatectomy, given recombinant human HGF via the portal vein, exhibited reduced extra-hepatic distribution and increased HGF content in liver tissues

Administration of recombinant human HGF via portal vein is suitable for patients with partial hepatectomy or recipients of LDLT. We therefore investigated the effect of 70% partial hepatectomy on HGF levels in the liver, spleen, and kidneys 5 min after the portal vein injection (Fig. 4). When 0.1 mg/kg HGF was injected via the portal vein in hepatectomized rats, the HGF content in liver, spleen, and kidneys increased to 1262.0 ± 616.6, 82.0 ± 18.3 and 38.5 ± 5.8 ng/g wet tissue, respectively, which is relatively higher than in normal rats (Fig. 2). Administration of a lower dose of recombinant HGF resulted in lower HGF content in liver, spleen, and kidneys. Interestingly, when 0.03 mg/kg of HGF was administered to 70% partial hepatectomized rats via the portal vein, the HGF content in liver tissues (547.8 ± 153.3 ng/g wet tissue) was approximately the same as that in normal rats administered with 0.1 mg/kg of the protein (Figs. 2 and 4). The

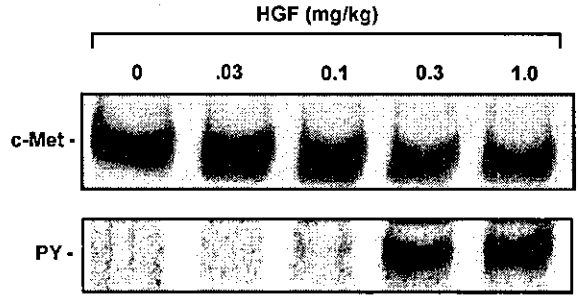

Fig. 3. Bolus injection of recombinant human HGF induced c-Met tyrosine phosphorylation in liver tissue. Recombinant human HGF (0.03, 0.1, 0.3 and 1.0 mg/kg) or PBS was intravenously administered to normal rats. Liver tissues were obtained 30 min after bolus injection. Expression and tyrosine phosphorylation of c-Met were examined by Western blotting, as described in Section 2. Administration of more than 0.1 mg/kg of recombinant human HGF induced c-Met tyrosine phosphorylation in liver tissue, and expression of c-Met decreased in parallel with the dose of recombinant HGF.

dose of recombinant human HGF could be reduced to 30% to treat hepatectomized animals with a remnant liver volume of 30%. These results indicate that when recombinant human HGF is administered to patients with partial hepatectomy or recipients of LDLT, the protein dose should be modulated according to the remnant liver volume.

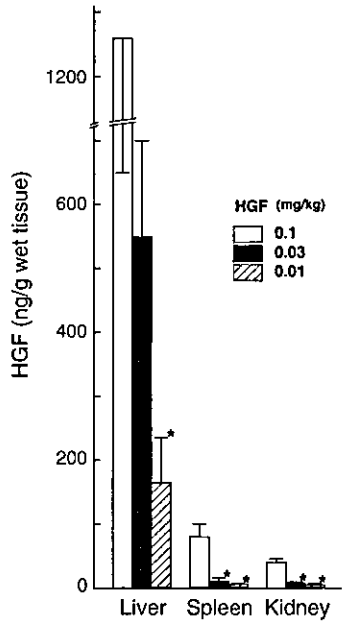

Fig. 4. Tissue distribution of recombinant human HGF administered via the portal vein to rats with 70% partial hepatectomy. Various doses of recombinant human HGF (0.01, 0.03 and 0.1 mg/kg) were administered to rats via the portal vein following 70% partial hepatectomy. The liver, spleen, and kidneys were obtained 5 min after injection, and tissue content of human HGF was measured by ELISA, as described in Section 2. Hepatectomized rats given 0.1 mg/kg of recombinant HGF exhibited an increase in hepatic and extra-hepatic distribution of the protein. When 70% hepatectomized rats were treated with 0.03 mg/kg of recombinant human HGF, its content in liver tissues (547.8 ± 153.3 ng/g wet tissue) was approximately the same as in normal rats given 0.1 mg/kg of recombinant HGF, as shown in Fig. 2. *, $P < 0.05$ in comparison with the HGF content in each organ of hepatectomized rats given recombinant human HGF (0.1 mg/kg).

4. Discussion

HGF is produced from mesenchymal cells as an inactive precursor, pro-HGF [27–29]. After tissue injury, pro-HGF is converted to an active heterodimer, consisting of light and heavy chains, primarily by a specific serine protease, HGF activator (HGFA) [30–32] as well as weakly by blood-coagulation factor XIIa [33]. Recently, HGFA inhibitor (HAI)-1, which was first identified as an inhibitor of HGFA [34], has been reported to act as a reservoir for HGFA in injured tissues [35]. Thus, HGF may play an important role in regeneration and repair of injured tissues, including the liver and intestine. In the present study, we investigated the pharmacokinetics of recombinant human HGF, the heterodimeric active form of HGF. Bolus injection of recombinant human HGF led to its distribution primarily to the liver and effectively induced c-Met tyrosine phosphorylation in liver. Therefore, despite its short half-life, it is possible that intravenously administered recombinant human HGF induces liver regeneration in patients with fatal liver disease. Indeed, intravenous bolus injection of recombinant HGF led to a considerable increase in serum HGF levels (Fig. 1). Treatment with this protein increased liver weight and serum albumin levels in a rat model of dimetylnitrosamine-induced liver injury, in which serum levels of endogenous rat HGF were increased to 2–3 ng/ml, (unpublished data), as well as following partial hepatectomy [36,37]. In addition, a single intravenous injection of recombinant human HGF rescued mice from anti-CD95-induced lethal hepatic failure via its anti-apoptotic effects (unpublished data), and HGF-induced inhibition of apoptosis has been reported in various models of hepatic injury, using HGF gene transfer or HGF protein [9–15]. Thus, when recombinant human HGF is administered to patients with fulminant hepatic failure, the treatment is thought to not only stimulate liver regeneration, but also inhibit disease progression through its anti-apoptotic activity.

When recombinant human HGF was administered intravenously to rats with 70% partial hepatectomy or CDAA diet-induced cirrhosis, serum levels of human HGF were elevated. These results suggest that extra-hepatic distribution of administered HGF is increased in patients with liver disease, leading to adverse side effects. Bolus injection of recombinant HGF actually induced considerable levels of HGF in renal tissue (Fig. 2). However, although HGF has been reported to ameliorate renal fibrosis and dysfunction [16], the repeated injection caused reversible proteinuria (unpublished data). Conversely, bolus injection via the portal vein was capable of delivering recombinant human HGF more specifically to the liver, reducing extra-hepatic distribution of the protein. Nevertheless, even when recombinant human HGF was administered via the portal vein, hepatectomized rats exhibited an increase in HGF levels in the liver, extra-hepatic tissues, and serum. Elevated human HGF contents in the remnant livers may be due to an increase in the amount of administered human HGF per liver volume, and it is possible that, once c-Met receptor and extracellular matrix in liver tissues are saturated, recombinant human HGF leads to an increase in human HGF levels in the serum and extra-hepatic tissues. Therefore, although intraportal injections are thought to reduce the effects on extra-hepatic organs, the dose of recombinant human HGF should be reduced according to the degree of liver injury or remnant liver volume regardless of the route of administration. Indeed, recombinant human HGF administered to rats with 70% partial hepatectomy could be reduced to 30% to achieve the same HGF level in liver tissues as in normal rats (Figs. 2 and 4).

HGF is also known to stimulate liver regeneration and reduce fibrosis in experimental models of liver cirrhosis [17–21], and administration of recombinant human HGF has the potential to become a new modality for cirrhosis patients. However, since lengthy HGF administration is likely required to treat cirrhotic patients, development of an appropriate drug delivery system for liver-specific targeting or long-term release is desirable. Additionally, the potential of HGF to stimulate hepatocellular carcinomas needs to be evaluated before beginning clinical applications.

HGF plays an important role in the repair of injured intestinal mucosa. We have recently reported that administration of recombinant human HGF, using osmotic pumps implanted into peritoneal cavities, resulted in a persistent increase in serum human HGF and facilitated colonic mucosal repair in a rat model of experimental colitis [38]. However, in the present study, the human HGF content of colon tissues was extremely low following intravenous injection of the recombinant protein. Therefore, it is necessary to explore whether repeated injections of human HGF ameliorate intestinal mucosal injury. Alternatively, tissue-specific delivery of the recombinant protein should be established to treat inflammatory bowel disease. Effectiveness of HGF has also been reported in animals with injury of various extra-hepatic organs, including kidney, lung, pancreas, and neurons [16,39–41]. Therefore, development of a delivery system for tissue-specific or long-term release may contribute to expanding the clinical application of recombinant human HGF to diseases of extra-hepatic organs, such as renal sclerosis, pulmonary fibrosis, severe pancreatitis, or neurodegenerative disease.

In conclusion, our findings presented here suggest that although recombinant HGF disappears rapidly from serum, bolus injection of recombinant human HGF may exert a therapeutic effect in patients with fatal liver disease.

Acknowledgements

We thank Ms. Sayoko Ohara and Ms. Kana Ohara for their technical assistance. This work was supported in part by grants-in-aid from the Ministry of Health, Labor and Welfare of Japan.

References

[1] Gohda E, Tsubouchi H, Nakayama H, et al. Human hepatocyte growth factor in plasma from patients with fulminant hepatic failure. Exp Cell Res 1986;166:139–50.

[2] Gohda E, Tsubouchi H, Nakayama H, et al. Purification and partial characterization of hepatocyte growth factor from plasma of a patient with fulminant hepatic failure. J Clin Invest 1988;81:414–9.

[3] Michalopoulos GK. Liver regeneration: molecular mechanisms of growth control. FASEB J 1990;4:176–85.

[4] Nagaike M, Hirao S, Tajima H, et al. Renotropic functions of hepatocyte growth factor in renal regeneration after unilateral nephrectomy. J Biol Chem 1991;266:22781–4.

[5] Dignass AU, Lynch-Devaney K, Podolsky DK. Hepatocyte growth factor/scatter factor modulates intestinal epithelial cell proliferation and migration. Biochem Biophys Res Commun 1994;202:701–9.

[6] Bussolino F, Di Renzo MF, Ziche M, et al. Hepatocyte growth factor is a potent angiogenic factor which stimulates endothelial cell motility and growth. J Cell Biol 1992;119:629–41.

[7] Zarneger R, Michalopoulos GK. The many faces of hepatocyte growth factor: from hepatopoiesis to hematopoiesis. J Cell Biol 1995;129:1177–80.

[8] Weidner KM, Sachs M, Birchmeier W. The met receptor tyrosine kinase transduces motility, proliferation, and morphogenic signals of scatter factor/hepatocyte growth factor in epithelial cells. J Cell Biol 1993;121:145–54.

[9] Okano J, Shiota G, Kawasaki H. Protective action of hepatocyte growth factor for acute liver injury caused by D-galactosamine in transgenic mice. Hepatology 1997;26:1241–9.

[10] Kosai K, Matsumoto K, Nagata S, Tsujimoto Y, Nakamura T. Abrogation of Fas-induced fulminant hepatic failure in mice by hepatocyte growth factor. Biochem Biophys Res Commun 1998;244:683–90.

[11] Masunaga H, Fujise N, Shiota A, et al. Preventive effects of the deleted form of hepatocyte growth factor against various liver injuries. Eur J Pharmacol 1998;342:267–79.

[12] Kosai K, Matsumoto K, Funakoshi H, Nakamura T. Hepatocyte growth factor prevents endotoxin-induced lethal hepatic failure. Hepatology 1999;30:151–9.

[13] Mori I, Tsuchida A, Taiji M, Noguchi H. Hepatocyte growth factor protects mice against anti-Fas antibody-induced death. Med Sci Res 1999;27:355–9.

[14] Nomi T, Shiota G, Isono M, Sato K, Kawasaki H. Adenovirus-mediated hepatocyte growth factor gene transfer prevents lethal liver failure in rats. Biochem Biophys Res Commun 2000;278:338–43.

[15] Xue F, Takahara T, Yata Y, et al. Attenuated acute liver injury in mice by naked hepatocyte growth factor gene transfer into skeletal muscle with electroporation. Gut 2002;50:558–62.

[16] Mizuno S, Kurosawa T, Matsumoto K, Mizuno-Horikawa Y, Okamoto M, Nakamura T. Hepatocyte growth factor prevents renal fibrosis and dysfunction in a mouse model of chronic renal disease. J Clin Invest 1998;101:1827–34.

[17] Yasuda H, Imai E, Shiota A, Fujise N, Morinaga T, Higashio K. Antifibrogenic effect of a deletion variant of hepatocyte growth factor on liver fibrosis in rats. Hepatology 1996;24:636–42.

[18] Matsuda Y, Matsumoto K, Yamada A, et al. Prevention and therapeutic effects in rats of hepatocyte growth factor infusion on liver fibrosis/cirrhosis. Hepatology 1997;26:81–9.

[19] Ueki T, Kaneda Y, Tsutsui H, et al. Hepatocyte growth factor gene therapy of liver cirrhosis in rats. Nat Med 1999;5:226–30.

[20] Sato M, Kakubari M, Kawamura M, Sugimoto J, Matsumoto K, Ishii T. The decrease in total collagen fibers in the liver by hepatocyte growth factor after formation of cirrhosis induced thioacetamide. Biochem Pharmacol 2000;59:681–90.

[21] Oe S, Fukunaka Y, Hirose T, Yamaoka Y, Tabata Y. A trial on regeneration therapy of rat liver cirrhosis by controlled release of hepatocyte growth factor. J Control Release 2003;307:146–51.

[22] Tsubouchi H, Niitani Y, Hirono S, et al. Levels of the human hepatocyte growth factor in serum of patients with various liver diseases determined by an enzyme-linked immunosorbent assay. Hepatology 1991;13:1–5.

[23] Tsubouchi H, Kawakami S, Hirono S, et al. Prediction of outcome in fulminant hepatic failure by serum human hepatocyte growth factor. Lancet 1992;340:307.

[24] Higgins GM, Anderson RM. Experimental pathology of the liver: restoration of the liver of the white rat following partial surgical removal. Arch Pathol 1931;12:186–202.

[25] Onaga M, Ido A, Hasuike S, et al. Enhanced expression of growth factors and imbalance between hepatocyte proliferation and apoptosis in the livers of rats fed a choline-deficient, L-amino acid-defined diet. Hepatol Res 2004;28:94–101.

[26] Kawakami S, Tsubouchi H, Nakagawa S, et al. Expression of hepatocyte growth factor in normal and carbon tetrachloride-treated monkeys. Hepatology 1994;20:1255–60.

[27] Gohda E, Kataoka H, Tsubouchi H, Daikuhara Y, Yamamoto I. Phorbol ester-induced secretion of human hepatocyte growth factor by human skin fibroblasts and its inhibition by dexamethasone. FEBS Lett 1992;301:107–10.

[28] Tamura M, Arakaki N, Tsubouchi H, Takada H, Daikuhara Y. Enhancement of human hepatocyte growth factor production by interleukin-1α ar-α by fibroblasts in culture. J Biol Chem 1993;268:8140–5.

[29] Gohda E, Takebe T, Sotani T, Nakamura S, Minowada J, Yamamoto I. Induction of hepatocyte growth factor by interleukin-γ in human leukemia cells. J Cell Physiol 1998;174:107–14.

[30] Miyazawa K, Shimomura T, Kitamura A, Kondo J, Morimoto Y, Kitamura N. Molecular cloning and sequence analysis of the cDNA for a human serine protease responsible for activation of hepatocyte growth factor. Structural similarity of the protease precursor to blood coagulation factor XII. J Biol Chem 1993;268:10024–8.

[31] Miyazawa K, Shimomura T, Naka D, Kitamura N. Proteolytic activation of hepatocyte growth factor in response to tissue injury. J Biol Chem 1994;269:8966–70.

[32] Miyazawa K, Shimomura T, Kitamura N. Activation of hepatocyte growth factor in the injured tissues is mediated by hepatocyte growth factor activator. J Biol Chem 1996;271:3615–8.

[33] Shimomura T, Miyazawa K, Komiyama Y, et al. Activation of hepatocyte growth factor by two homologous proteases, blood-coagulation factor XIIa and hepatocyte growth factor activator. Eur J Biochem 1995;229:257–61.

[34] Shimomura T, Denda K, Kitamura A, et al. Hepatocyte growth factor activator inhibitor, a novel Kunitz-type serine protease inhibitor. J Biol Chem 1997;272:6370–6.

[35] Kataoka H, Shimomura T, Kawaguchi T, et al. Hepatocyte growth factor activator inhibitor type-1 is a specific cell surface binding protein of hepatocyte growth factor activator (HGFA) and regulates HGFA activity in the pericellular microenvironment. J Biol Chem 2000;275:40453–62.

[36] Fujiwara K, Nagoshi S, Ohno A, et al. Stimulation of liver growth by exogenous human hepatocyte growth factor in normal and partially hepatectomized rats. Hepatology 1993;18:1443–9.

[37] Ishii T, Sato M, Sudo K, et al. Hepatocyte growth factor stimulates liver regeneration and elevates blood protein levels in normal and partially hepatectomized rats. J Biochem 1995;117:1105–12.

[38] Tahara Y, Ido A, Yamamoto S, et al. Hepatocyte growth factor facilitates colonic mucosal repair in experimental ulcerative colitis in rats. J Pharmacol Exp Ther 2003;307:146–51.

[39] Dohi M, Hasegawa T, Yamamoto K, Marshall BC. Hepatocyte growth factor attenuates collagen accumulation in a murine model of pulmonary fibrosis. Am J Respir Crit Care Med 2000;162:2302–7.
[40] Warzecha Z, Dembinski A, Konturek PC, et al. Hepatocyte growth factor attenuates pancreatic damage in cerulein-induced pancreatitis in rats. Eur J Pharmacol 2001;430:113–21.
[41] Sun W, Funakoshi H, Nakamura T. Overexpression of HGF retards disease progression and prolongs life span in a transgenic mouse model of ALS. J Neurosci 2002;22:6537–48.

Review TRENDS in Microbiology Vol.12 No.8 August 2004

The role of Paneth cells and their antimicrobial peptides in innate host defense

Tokiyoshi Ayabe[1], Toshifumi Ashida[1], Yutaka Kohgo[1] and Toru Kono[2]

[1]Department of Internal Medicine III, Asahikawa Medical College, 2-1-1-1 Midorigaoka-Higashi, Asahikawa 078-8510, Japan
[2]Department of Surgery II, Asahikawa Medical College, 2-1-1-1 Midorigaoka-Higashi, Asahikawa 078-8510, Japan

The intestinal epithelium is the largest surface area that is exposed to various pathogens in the environment, however, in contrast to the colon the number of bacteria that colonize the small intestine is extremely low. Paneth cells, one of four major epithelial cell lineages in the small intestine, reside at the base of the crypts and have apically oriented secretory granules. These granules contain high levels of antimicrobial peptides that belong to the α-defensin family. Paneth cells secrete these microbicidal granules that contain α-defensins when exposed *ex vivo* to bacteria or their antigens, and recent evidence reveals that antimicrobial peptides, particularly α-defensins, that are present in Paneth cells contribute to intestinal innate host defense.

Multicellular organisms use various strategies to protect themselves against microbes. In mammals, the immune system is the host's defense against possible pathogens and consists of innate and adaptive immune mechanisms. Adaptive immunity, which is only found in vertebrates, is well characterized. By contrast, innate immunity is not considered as a vital defense system because it is thought to consist of only passive, non-specific reactions. It is known that non-vertebrates, such as insects and plants, produce antimicrobial peptides (AMPs) and that these are the effectors of the innate immune response [1–3]. Vertebrates, ranging from fish and frogs to humans, also produce these endogenous AMPs [4–7].

A continuous monolayer of gastrointestinal epithelial cells functions as the primary physical barrier against microbial invasion. There is much evidence to support the hypothesis that a variety of epithelia are actively involved in the innate host defense [8]. In intestinal epithelia, Paneth cells are the producers of AMPs [9–11]. Recent analyses of the molecular mechanisms that AMPs and pattern recognition molecules use in innate immunity have illustrated that this type of immune response is a vital, evolutionarily conserved and complex system for responding to microbial infection [12–14]. AMPs, especially defensins, are summarized in Box 1 (see also Table 1). In this review, recent advances in understanding the roles of Paneth cells and their AMPs in innate host defense will be discussed and summarized.

Innate immunity in intestinal mucosa

The mammalian intestinal epithelium is the largest host surface area that is exposed to pathogens. It is well known that the number of bacteria that colonize the small intestine is extremely low relative to that found in the colon. Factors that result in the low bacterial numbers of the small intestinal lumen include barriers such as intestinal motility, digestive juice, mucus or the immune cell response (Box 2). The role of adaptive immunity in small intestinal responses to infection has been vigorously studied, particularly with respect to the contribution of gut-associated lymphoid tissue, γδ-T cells or cytokines, such as interleukin (IL)-2, IL-7 and IL-18 [15–17]. By contrast, the concept that innate immunity is a key component of the small intestinal barrier had not received extensive consideration until recently. Phagocytes that migrate from circulation and reside in the lamina propria probably have a role in the removal of invasive microbes. In addition, the small intestine is known to contain AMPs

Box 1. Defensins as antimicrobial peptides (AMPs)

Antimicrobial peptides (AMPs) are small peptides, usually consisting of less than 40 amino acids, which have a broad spectrum of microbicidal activities against Gram-negative and Gram-positive bacteria, fungi, protozoa and even enveloped viruses [13]. More than 500 AMPs have been discovered, and because of their structural diversity they have been classified on the basis of their secondary structure: magainins and numerous cathelicidins contain an α-helical structure, defensins have a β-sheet that contains three disulphide bonds, and a cathelicidine, known as PR-39, has a linear non-α-helical structure [46–50].

Defensins consist of cationic AMP families: α-defensins, β-defensins and θ-defensins. Defensin peptides function in a non-oxidative microbicidal manner against a variety of microbes. The α-defensins were among the first AMP families to be characterized, having been defined as major constituents of the primary granules of mammalian phagocytic leukocytes [51]. In addition, α-defensins are abundant in cytosolic granules of Paneth cells in human and mouse small intestine [9,10]. Amino acid sequences of some mouse and human α-defensins are shown in Table 1 in the main text. β-defensins are more widely expressed, being detected in neutrophils, airway epithelium, kidney, pancreas, salivary gland, skin and on every mucosal surface that has been investigated [51–53]. The first circular peptide to be discovered in the animal kingdom was the θ-defensin that is found in primate neutrophils; this defensin is a potent salt-insensitive microbicidal molecule [54].

Corresponding author: Tokiyoshi Ayabe (ayabe@asahikawa-med.ac.jp).

www.sciencedirect.com 0966-842X/$ - see front matter doi:10.1016/j.tim.2004.06.007

Table 1. Amino acid sequences of α-defensins in mouse and human

In mouse Paneth cells	
Cryptdin-1	LRDLVCYCRSRGCKGRERMNGTCRKGHLLYTLCCR
Cryptdin-2	LRDLVCYCRTRGCKRRERMNGTCRKGHLMYTLCCR
Cryptdin-3	LRDLVCYCRKRGCKRRERMNGTCRKGHLMYTLCCR
Cryptdin-4	GLLCYCRKGHCKRGERVRGTC-G-IRFLYCCPRR
Cryptdin-5	LSKKLICYCRIRGCKRRERVFGTCRNLFLTFVFCCS
Cryptdin-6	LRDLVCYCRARGCKGRERMNGTCRKGHLLYMLCCR
In human neutrophils (HNP-1 ~ HNP-4) and Paneth cells (HD5 and HD6)	
HNP-1	ACYCRIPACIAGERRYGTCIYQGRLWAFCC
HNP-2	CYCRIPACIAGERRYGTCIYQGRLWAFCC
HNP-3	DCYCRIPACIAGERRYGTCIYQGRLWAFCC
HNP-4	VCSCRLVFCRRTELRVGNCLIGGVSFTYCCTRVD
HD5	ATCYCRTGRCATRESLSGVCEISGRLYRLCCR
HD6	AFTCHCRRS-CYSTEYSYGTCTVMGINHRFCCL

that might contribute to the innate immunity against microbial colonization.

The intestinal epithelium is continually renewed throughout mammalian life, as the progeny of stem cells migrate from their site of origin in crypts upward onto villi, during which time they differentiate into columnar cells, enteroendocrine cells or goblet cells. In contrast to these three epithelial lineages, Paneth cells [18] migrate downward from the stem cell zone toward the base of the crypt. Evidence from many lines of investigation support the hypothesis that the release of AMPs by epithelial cells contributes to innate mucosal immunity. In the small intestine, only Paneth cells appear to contain and release AMPs. M cells are known to exist in gut-associated lymphoid tissue, and pathogens or allergens are taken via M cells and presented to lymphocytes. This is an example of crosstalk between innate and adaptive immunity in the gut.

The role of Paneth cells in host defense

Paneth cells at the base of crypts in the small intestine contain lysozyme, secretory phospholipase A_2 and α-defensins in secretory granules, all of which have *in vitro* antimicrobial activities [19,20]. In contrast to villus enterocytes that have a lifetime of 2–3 days, Paneth cells live for more than 20 days and are renewed at a slower rate. In certain abnormal inflammatory conditions, Paneth cell-like cells can be found ectopically, such as in the colon during inflammatory bowel disease or in the pancreas during chronic pancreatitis [21]. The roles of tumor necrosis factor (TNF)-α, NOD2, CD95 ligand and zinc-binding proteins in Paneth cells are not understood, but their presence suggests that Paneth cell secretions might influence many different activities in the microenvironment of the crypt [22–24]. Recently, NOD2 expression in Paneth cells of both normal and Crohn's disease patients was reported [25].

Box 2. Factors involved in barrier functions for gastrointestinal tract

- Low pH of gastric juice
- Mucus
- Intestinal motility
- Tight junctions
- Regeneration of epithelial cells
- Antimicrobial peptides (e.g. defensins)
- Antimicrobial proteins (e.g. lysozyme and lactoferrin)
- Paneth cells
- Phagocytic cells
- Lymphocytes
- Antibodies
- Gut-associated lymphoid tissues
- M cells
- Normal flora

Paneth cell α-defensins, cryptdins in mice, and HD5 and HD6 in humans are antimicrobial constituents of apically oriented granules that have been shown to exhibit potent antimicrobial activities against microorganisms (including Gram-positive and Gram-negative bacteria, fungi and protozoa) in assays *in vitro* [26]. They have been recovered from intact tissue and from the lumen of the small intestine. As typical α-defensin family peptides, cryptdins are cationic peptides ranging from 3 to 4 kilodaltons in size. Six cryptdin peptides, cryptdin-1 to cryptdin-6, have been isolated and characterized in mice.

Satoh *et al.* [27,28] concluded from microscopic observations that *in vivo* fecal administration to the ileum induced morphological changes in Paneth cells in rat small intestine. When small intestinal crypts were stimulated *in vitro* by a cholinergic secretagogue, the Ca^{2+} dynamics were detected exclusively in Paneth cells [29]. Garabedian *et al.* [30] have shown that mice transgenic for attenuated diphtheria toxin A, which is expressed under the direction of the mouse cryptdin-2 gene promoter (CR2-tox), were deficient in mature Paneth cells. Because CR2-tox mice exhibited no phenotype in a conventional specific pathogen-free environment, the authors suggested that antimicrobial factors produced by Paneth cells are not required to prevent microbial colonization in a laboratory setting. However, because of the transient Paneth cell deficiency phenotype in CR2-tox mice, the function of Paneth cells and the role of their AMPs remain to be defined.

Proteolytic activation is required for precursors of α-defensin peptides to have microbicidal activity. In mouse small intestine, matrix metalloproteinase-7 (MMP-7, also known as matrilysin) colocalizes with cryptdins in Paneth cell granules and is the processing enzyme for procryptdins. Wilson *et al.* [31] showed that MMP-7-deficient mice, which lack mature cryptdins, exhibited decreased antimicrobial activity against orally administered bacteria *in vivo*, and were more susceptible to oral *Salmonella* infection than wild-type mice [31]. This was the first evidence that AMPs derived from Paneth cells contribute to the innate enteric host defense *in vivo*. In mice, the activation of cryptdin peptides by MMP-7 primarily occurs before secretion [32]. In human Paneth cells, a trypsin expressed in Paneth cell granules processes HD5. However, activation of HD5 occurs at secretion or shortly thereafter, because mature HD5 is not detected in Paneth cells [33].

In contrast to mice, human Paneth cells lack MMP-7. Human Paneth cells release the α-defensin HD5 precursor, $proHD5_{(20-94)}$, into the small intestinal lumen, which is then processed rapidly after secretion by anionic and/or meso isoforms of trypsin [34,35]. The trypsin cleavage site

in proHD5$_{(20-94)}$ lies between residues R62 and A63 and gives rise to the major form of the mature peptide found in washes of the small intestinal lumen [33]. The differences between mouse and human α-defensin processing suggest that the capacity for releasing mature microbicidal α-defensins is conserved, but that differing mechanisms have evolved to ensure the delivery of functional peptides into the lumen.

Microbicidal secretions by Paneth cells in response to bacteria

Paneth cells secrete α-defensins and other granule constituents in response to carbamyl choline, bacteria or their antigens, such as lipopolysaccharide (LPS) and muramyl dipeptide [35]. In mice, cryptdins constitute the majority of antimicrobial activity in Paneth cell secretions. Although the mechanisms are not known, the observation that bacteria induce Paneth cell secretion selectively suggests that a regulated pathway links bacterial recognition to the exocytotic apparatus. As illustrated in Figure 1, these recent studies have defined the role of the Paneth cell in innate enteric immunity and have established a new role of mucosal immunity at the intestinal epithelial surface. The Ca^{2+}-activated potassium channel, *mIKCa1*, is Paneth cell-specific in mouse small intestinal epithelium and functions in the secretory response of Paneth cells to bacteria [32]. For example, *IKCa1* channel-specific blockers inhibited LPS-induced release of cryptdins by Paneth cells in a dose-dependent manner [36]. Studies using mice transgenic for HD5, which express human Paneth cell α-defensin, showed that HD5 in mouse Paneth cells is highly protective against an orally administered lethal dose of virulent *Salmonella* [37]. These findings further confirm that Paneth cell α-defensins contribute to innate enteric immunity. To date, there is no evidence to suggest how Paneth cells recognize individual bacteria. Although Paneth cells might not selectively recognize differences between commensal or virulent bacteria, they do recognize bacterial factors [35]. Paneth cells are responsible for maintaining the homeostasis of the villus–crypt microenvironment by controlling the portal of microbes.

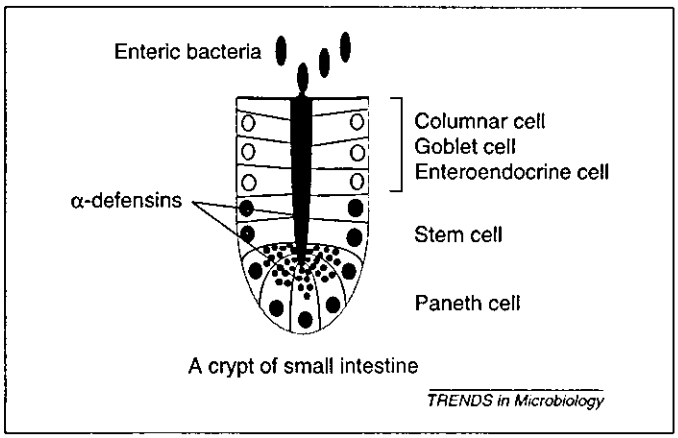

Figure 1. Secretion of microbicidal α-defensins by Paneth cells in response to bacteria. Small intestinal Paneth cells contribute to mucosal innate host defense by sensing bacteria or bacterial antigens, such as lipopolysaccharide, and secreting microbicidal peptides, particularly α-defensins [35].

The contribution of Paneth cell α-defensins to enteric mucosal immunity is most evident from the phenotype of mice transgenic for the human Paneth cell α-defensin HD5 (tg-HD5) [37]. These tg-HD5 mice specifically express the human minigene in Paneth cells and are completely immune to oral infection by *Salmonella enterica* serovar Typhimurium, even when challenged orally with an inoculum that is 1×10^4 times the LD_{50} (lethal dose 50). Recently, recombinant HD5 and mouse cryptdins have been found to have similar bactericidal activities against wild-type *S. typhimurium* (H. Tanabe, A.J. Ouellette and C.L. Bevans, unpublished), dispelling the view that immunity to *Salmonella* results from the introduction of a peptide with superior bactericidal activity. Perhaps the presence of HD5 in mouse Paneth cell secretions modifies the composition of the microflora by unknown selective means, conferring greater resistance to *S. typhimurium*.

A recent report has presented evidence that oral inoculation of mice with wild-type *S. typhimurium* decreased levels of cryptdin mRNAs and peptides [38]. Interestingly, inoculation with attenuated *Salmonella* serovar Typhimurium strains and strains lacking the SPI1 type III secretion system, or *Listeria monocytogenes*, did not modulate cryptdin levels. The authors speculated that the observed effects could have resulted from direct interactions between *Salmonella* and Paneth cells or from the effects of *Salmonella* on villous enterocytes, therefore leading to induced release of mediators from the enterocytes via a p38-signaling pathway. It will be of interest to discern the molecular and cellular details of these events in the gut and to test whether tg-HD5 mice exhibit a similar downregulation of cryptdin gene expression.

Future perspectives

Much of Paneth cell biology and the role or responses of Paneth cells and their AMPs to immunopathologies remain open questions. For instance, the stem cells that continuously renew the small intestinal epithelia have not been identified or isolated. Therefore, the mechanisms that regulate transcription and signaling in regeneration and differentiation of individual cell lineages of the small intestine, including Paneth cells, remain obscure. The relationship between several diseases and AMPs has been reported. Among them, the β-defensin dysfunction in patients with cystic fibrosis and the protective role of a cathelicidin (LL37) against skin infections have been described [39–42]. In the intestine, associations exist between Paneth cell α-defensins and necrotizing enterocolitis in immature babies, but causal relations have not been established [43]. In Crohn's disease, mutations in the NOD2 gene (involved in cytoplasmic recognition of bacterial antigens) correlates with susceptibility to the disease [44,45]. Paneth cells express NOD2 in the small intestinal crypts of both healthy volunteers and patients with Crohn's disease [23]. Because NOD2 is not a membrane-bound molecule but a cytoplasmic molecule, it might not be a direct target for bacterial recognition. To clarify the signal transduction molecules that are associated with bacterial recognition in Paneth cells, intact Paneth cells are now tested at the single cell level. On the basis of current information regarding molecules found in

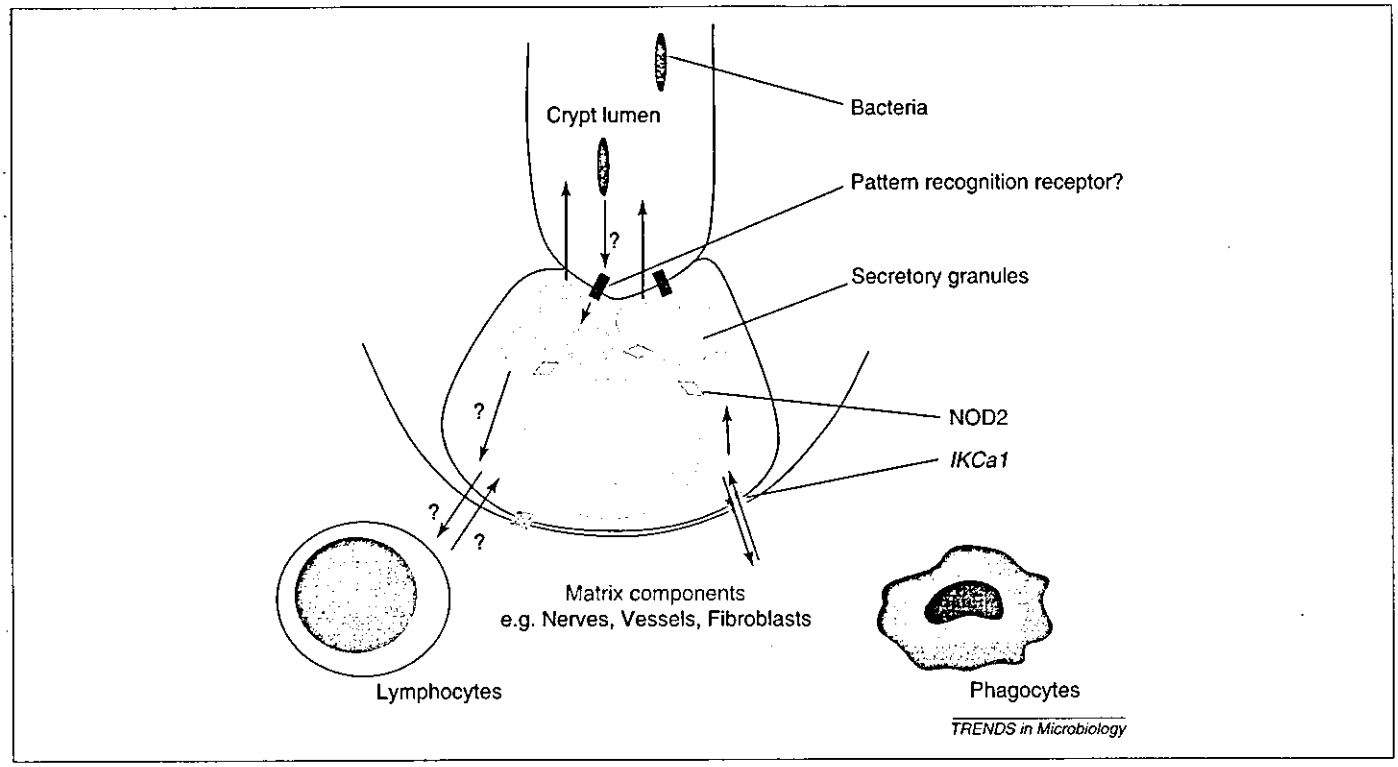

Figure 2. Possible biological and immunological responses via Paneth cells. Paneth cells reside in the bottom of small intestinal crypts and might regulate certain biological and immunological small intestinal responses. Secretory granules contain many bioactive factors. Crosstalks between microbes and Paneth cells, and between Paneth cells and matrix components, including cells in adaptive immunity and mesenchymal cells, might take place in the crypt microenvironment.

Paneth cells as well as hypothetical molecules, Figure 2 describes the possibilities for crosstalk between microbes and Paneth cells, and between Paneth cells and matrix components, including cells involved in the adaptive immune response and mesenchymal cells. Residing in the bottom of crypts, Paneth cells might regulate certain biological and immunological small intestinal responses. Alternatively, these cells might arise in greater numbers during inflammatory episodes to provide higher local levels of α-defensins in response to the possibility of increased infectious threat.

The use of antibiotics saves a lot of human lives from many serious infections. Even so, there are disadvantages associated with such usage, including the increase in the number of multiple antibiotic-resistant microbes, the high rate of opportunistic infections that are appearing in hospitals and also cost-benefit issues. Some advantages for the use of AMPs can be highlighted by mechanisms that do not result in microbial resistance compared with the use of antibiotics, and also the relative safety of their use because they are host-endogenous peptides. In the USA, efforts have already commenced to investigate the potential use of AMPs in the treatment of infectious diseases or complications caused by pathogens that are resistant to conventional antibiotics.

Concluding remarks

Innate immunity plays a crucial role in intestinal host defense. The epithelial innate host defense is not a passive nonspecific process, but a potent well-regulated system. The molecular basis of signaling molecules in innate enteric immunity and possible pathological contributions of Paneth cells and their AMPs to human diseases has attracted increasing attention. The time might be opportune for testing cohorts of patients for evidence of genomic or proteomic polymorphisms that could alter the synthesis, function or delivery of innate immune mediators by this unique epithelial cell.

Acknowledgements

We thank A.J. Ouellette (University of California, Irvine, College of Medicine) for useful discussions. This paper is supported partially by Grant-in-Aid for Scientific Research on Priority Areas (C) from The Ministry of Education, Culture, Sports, Science (TA*) and Technology in Japan, and Industrial Technology Research Grant Program in #02A02013a from New Energy and Industrial Technology Development Organization of Japan (TA*).

References

1 Steiner, H. *et al.* (1981) Sequence and specificity of two antibacterial proteins involved in insect immunity. *Nature* 292, 246–268
2 Broekaert, W.F. *et al.* (1995) Plant defensins: novel antimicrobial peptides as components of the host defense system. *Plant Physiol.* 108, 1353–1358
3 Metz-Boutigue, M.H. *et al.* (2003) Innate immunity: involvement of new neuropeptides. *Trends Microbiol.* 11, 585–592
4 Cole, A.M. *et al.* (1997) Isolation and characterization of pleurocidin, an antimicrobial peptide in the skin secretions of winter flounder. *J. Biol. Chem.* 272, 12008–12013
5 Zasloff, M. (1987) Magainins, a class of antimicrobial peptides from *Xenopus* skin: isolation, characterization of two active forms, and partial cDNA sequence of a precursor. *Proc. Natl. Acad. Sci. U. S. A.* 84, 5449–5453
6 Selsted, M.E. *et al.* (1985) Primary structure of three human neutrophil defensins. *J. Clin. Invest.* 76, 1436–1439
7 Ganz, T. and Lehrer, R.I. (1998) Antimicrobial peptides of vertebrates. *Curr. Opin. Immunol.* 10, 41–44
8 Schonwetter, B.S. *et al.* (1995) Epithelial antibiotics induced at sites of inflammation. *Science* 267, 1645–1648

9 Ouellette, A.J. *et al.* (1994) Mouse Paneth cell defensins: primary structures and antibacterial activities of numerous cryptdin isoforms. *Infect. Immun.* 62, 5040–5047
10 Jones, D.E. and Bevins, C.L. (1992) Paneth cells of the human small intestine express an antimicrobial peptide gene. *J. Biol. Chem.* 267, 23216–23225
11 Hooper, L.V. *et al.* (2003) Angiogenins: a new class of microbicidal proteins involved in innate immunity. *Nat. Immunol.* 4, 269–273
12 Medzhitov, R. *et al.* (1997) A human homologue of the *Drosophila* Toll protein signals activation of adaptive immunity. *Nature* 388, 394–397
13 Akira, S. *et al.* (2001) Toll-like receptors: critical proteins linking innate and acquired immunity. *Nat. Immunol.* 2, 675–680
14 Takeda, K. *et al.* (2003) Toll-like receptors. *Annu. Rev. Immunol.* 21, 335–376
15 Sadlack, B. *et al.* (1993) Ulcerative colitis-like disease in mice with a disrupted interleukin-2 gene. *Cell* 75, 253–261
16 Watanabe, M. *et al.* (1995) Interleukin-7 is produced by human intestinal cells and regulates the proliferation of intestinal mucosal lymphocytes. *J. Clin. Invest.* 95, 2945–2953
17 Kanai, T. *et al.* (2001) Macrophage-derived IL-18-mediated intestinal inflammation in the murine model of Crohn's disease. *Gastroenterology* 121, 875–888
18 Paneth, J. (1888) Ueber die secernierenden Zellen des Duenndarmepithels. *Archiv. Mikr. Anat.* 31, 113–191
19 Ouellette, A.J. (1997) Paneth cells and innate immunity in the crypt microenvironment. *Gastroenterology* 113, 1779–1784
20 Porter, E.M. *et al.* (1997) Broad-spectrum antimicrobial activity of human intestinal defensin 5. *Infect. Immun.* 65, 2396–2401
21 Stamp, G.W. *et al.* (1992) Lysozyme gene expression in inflammatory bowel disease. *Gastroenterology* 103, 532–538
22 Keshav, S. *et al.* (1990) Tumor necrosis factor mRNA localized to Paneth cells of normal murine intestinal epithelium by *in situ* hybridization. *J. Exp. Med.* 171, 327–332
23 Morita, Y. *et al.* (2001) Identification of xanthine dehydrogenase/xanthine oxidase as a rat Paneth cell zinc-binding protein. *Biochim. Biophys. Acta* 1540, 43–49
24 Porter, E.M. *et al.* (2002) The multifaceted Paneth cell. *Cell. Mol. Life Sci.* 59, 156–170
25 Lala, S. *et al.* (2003) Crohn's disease and the NOD2 gene: a role for paneth cells. *Gastroenterology* 125, 47–57
26 Ouellette, A.J. and Bevins, C.L. (2001) Paneth cell defensins and innate immunity of the small bowel. *Inflamm. Bowel Dis.* 7, 43–50
27 Satoh, Y. *et al.* (1986) Quantitative light microscopic observations on Paneth cells of germ-free and ex-germ-free Wistar rats. *Digestion* 34, 115–121
28 Satoh, Y. and Vollrath, L. (1986) Quantitative electron microscopic observations on Paneth cells of germfree and ex-germfree Wistar rats. *Anat. Embryol.* 173, 317–322
29 Satoh, Y. *et al.* (1995) Carbamylcholine- and catecholamine-induced intracellular calcium dynamics of epithelial cells in mouse ileal crypts. *Gastroenterology* 108, 1345–1356
30 Garabedian, E.M. *et al.* (1997) Examining the role of Paneth cells in the small intestine by lineage ablation in transgenic mice. *J. Biol. Chem.* 272, 23729–23740
31 Wilson, C.L. *et al.* (1999) Regulation of intestinal α-defensin activation by the metalloproteinase matrilysin in innate host defense. *Science* 286, 113–117
32 Ayabe, T. *et al.* (2002) Activation of Paneth cell α-defensins in mouse small intestine. *J. Biol. Chem.* 277, 5219–5228
33 Ghosh, D. *et al.* (2002) Paneth cell trypsin is the processing enzyme for human defensin-5. *Nat. Immunol.* 3, 583–590
34 Cunliffe, R.N. *et al.* (2001) Human defensin 5 is stored in precursor form in normal Paneth cells and is expressed by some villous epithelial cells and by metaplastic Paneth cells in the colon in inflammatory bowel disese. *Gut* 48, 176–185
35 Ayabe, T. *et al.* (2000) Secretion of microbicidal -defensins by intestinal Paneth cells in response to bacteria. *Nat. Immunol.* 1, 113–118
36 Ayabe, T. *et al.* (2002) Modulation of mouse Paneth cell α-defensin secretion by mIKCa1, a Ca^{2+}-activated, intermediate conductance Potassium channel. *J. Biol. Chem.* 277, 3793–3800
37 Salzman, N.H. *et al.* (2003) Protection against enteric salmonellosis in transgenic mice expressing a human intestinal defensin. *Nature* 422, 522–526
38 Salzman, N.H. *et al.* (2003) Enteric *Salmonella* infection inhibits Paneth cell antimicrobial peptide expression. *Infect. Immun.* 71, 1109–1115
39 Smith, J.J. *et al.* (1996) Cystic fibrosis airway epithelia fail to kill bacteria because of abnormal airway surface fluid. *Cell* 85, 229–236
40 Goldman, M.J. *et al.* (1997) Human β-defensin-1 is a salt-sensitive antibiotic in lung that is inactivated in cystic fibrosis. *Cell* 88, 553–560
41 Nizet, V. *et al.* (2001) Innate antimicrobial peptide protects the skin from invasive bacterial infection. *Nature* 414, 454–457
42 Ong, P.Y. *et al.* (2002) Endogenous antimicrobial peptides and skin infections in atopic dermatitis. *N. Engl. J. Med.* 347, 1151–1160
43 Salzman, N.H. *et al.* (1998) Enteric defensin expression in necrotizing enterocolitis. *Pediatr. Res.* 44, 20–26
44 Hugot, J.P. *et al.* (2001) Association of NOD2 leucine-rich repeat variants with susceptibility to Crohn's disease. *Nature* 31, 599–603
45 Ogura, Y. *et al.* (2001) A frameshift mutation in NOD2 associated with susceptibility to Crohn's disease. *Nature* 31, 603–606
46 Kisich, K.O. (2001) Antimycobacterial agent based on mRNA encoding human β-Defensin 2 enables primary macrophages to restrict growth of Mycobacterium tuberculosis. *Infect. Immun.* 69, 2692–2699
47 Bals, R. (1999) Augmentation of innate host defense by expression of a cathelicidin antimicrobial peptide. *Infect. Immun.* 67, 6084–6089
48 Bechinger, B. *et al.* (1993) Structure and orientation of the antibiotic peptide magainin in membranes by solid-state nuclear magnetic resonance spectroscopy. *Protein Sci.* 2, 2077–2084
49 Maloy, W.L. and Kari, U.P. (1995) Structure-activity studies on magainins and other host defense peptides. *Biopolymers* 37, 105–122
50 Matsuzaki, K. (1999) Why and how are peptide-lipid interactions utilized for self-defense? Magainins and tachyplesins as archetypes. *Biochim. Biophys. Acta* 1462, 1–10
51 Ouellette, A.J. and Selsted, M.E. (1996) Paneth cell defensins: endogenous peptide components of intestinal host defense. *FASEB J.* 10, 1280–1289
52 Zasloff, M. (2002) Antimicrobial peptides of multicellular organisms. *Nature* 415, 389–395
53 Selsted, M.E. *et al.* (1992) Indolicidin, a novel bactericidal tridecapeptide amide from neutrophils. *J. Biol. Chem.* 267, 4292–4295
54 Tang, Y.Q. *et al.* (1999) A cyclic antimicrobial peptide produced in primate leukocytes by the ligation of two truncated alpha-defensins. *Science* 286, 498–502

Oncogene (2004) 23, 7416–7429

www.nature.com/onc

TGF-β and HGF transmit the signals through JNK-dependent Smad2/3 phosphorylation at the linker regions

Shigeo Mori[1], Koichi Matsuzaki*[,1], Katsunori Yoshida[1], Fukiko Furukawa[1], Yoshiya Tahashi[1], Hideo Yamagata[1], Go Sekimoto[1], Toshihito Seki[1], Hirofumi Matsui[2,3], Mikio Nishizawa[4], Jun-ichi Fujisawa[5] and Kazuichi Okazaki[1]

[1]*Third Department of Internal Medicine, Kansai Medical University, 10-15 Fumizonocho, Moriguchi, Osaka 570-8507, Japan;* [2]*Division of Gastroenterology, Institute of Clinical Medicine, University of Tsukuba, 2-1-1 Amakubo, Tsukuba, Ibaraki 305-8576, Japan;* [3]*RIKEN Cell Bank, The Institute of Chemistry and Physics (RIKEN), 3-1-1 Koyadai, Tsukuba, Ibaraki 305-0074, Japan;* [4]*Department of Medical Chemistry, Kansai Medical University, 10-15 Fumizonocho, Moriguchi, Osaka 570-8507, Japan;* [5]*Department of Microbiology, Kansai Medical University, 10-15 Fumizonocho, Moriguchi, Osaka 570-8507, Japan*

Although hepatocyte growth factor (HGF) can act synergistically or antagonistically with transforming growth factor-β (TGF-β) signaling, molecular mechanism of their crosstalk remains unknown. Using antibodies which selectively distinguished receptor-regulated Smads (R-Smads) phosphorylated at linker regions from those at C-terminal regions, we herein showed that either HGF or TGF-β treatment of normal stomach-origin cells activated the JNK pathway, thereafter inducing endogenous R-Smads phosphorylation at linker regions. However, the phosphorylation at their C-terminal regions was not induced by HGF treatment. The activated JNK could directly phosphorylate R-Smads *in vitro* at the same sites that were phosphorylated in response to TGF-β or HGF *in vivo*. Thus, the linker regions of R-Smads were the common phosphorylation sites for HGF and TGF-β signaling pathways. The phosphorylation induced by simultaneous treatment with HGF and TGF-β allowed R-Smads to associate with Smad4 and to translocate into the nucleus. JNK pathway involved HGF and TGF-β-mediated infiltration potency since a JNK inhibitor SP600125 caused the reduction of invasive capacity induced by HGF and TGF-β signals. Moreover, a combined treatment with HGF and TGF-β led to a potent increase in plasminogen activator inhibitor type 1 transcriptional activity through Smad3 phosphorylation at the linker region. In contrast, HGF treatment reduced TGF-β-dependent activation of $p15^{INK4B}$ promoter, in which Smad3 phosphorylation at the C-terminal region was involved. In conclusion, HGF and TGF-β transmit the signals through JNK-mediated R-Smads phosphorylation at linker regions.
Oncogene (2004) **23**, 7416–7429. doi:10.1038/sj.onc.1207981
Published online 23 August 2004

Keywords: TGF-β; HGF; JNK; MAPK; Smad; PAI-1

*Correspondence: K Matsuzaki; E-mail: matsuzak@takii.kmu.ac.jp
Received 13 November 2003; revised 4 June 2004; accepted 4 June 2004; published online 23 August 2004

Introduction

Transforming growth factor-β (TGF-β) belongs to a family of multifunctional cytokines that participates not only in tumor suppressor activities such as growth inhibition, but also in oncogenic activities such as growth stimulation, increased motility and invasiveness (Roberts and Sporn, 1990).

Recent studies have elucidated how TGF-β initiates its response (Massagué, 1998). TGF-β binds to and activates two different transmembrane receptor serine/threonine kinases. Receptor-activated Smads (R-Smads) such as Smad2 and Smad3 are phosphorylated by the activated TGF-β type I receptor (TβRI) on the C-terminal SSXS motif (Macías-Silva *et al.*, 1996). The activated R-Smads form the complex with the common partner Smad4, and are translocated into the nucleus (Heldin *et al.*, 1997). The heteromeric Smad complex interacts with other transcription factors at regulatory promoter sequences of target genes (Derynck *et al.*, 1998), and recruits coactivators or corepressors to regulate the transcription of the specific genes, positively or negatively (Wrana, 2000a). R-Smads and Smad4 contain two highly conserved domains, the Mad homology (MH) 1 domains and the MH2 domains, which are connected by middle linker regions (Massagué, 1998). Whereas their MH1 domains can interact with the DNA, the MH2 domains are endowed with transcriptional activation properties. In addition to these Smads, Smad7 induced by TGF-β blocks the phosphorylation of R-Smads by acting as a pseudo-substrate for TβRI (Nakao *et al.*, 1997).

In contrast to TGF-β family ligands, hepatocyte growth factor (HGF) and epidermal growth factor (EGF) signal their responses through transmembrane receptor tyrosine kinases (Schlessinger, 2002). Multiple signaling pathways that originate from these receptors have been identified. The most prominent pathways are mediated by mitogen-activated protein kinases (MAPKs); extracellular signal-regulated protein kinase (ERK), c-Jun N-terminal kinase/stress-activated protein

kinase-1 (JNK/SAPK1), and stress-activated protein kinase-2 (p38), which in turn activate several transcription factors (Robinson and Cobb, 1997). Notably, TGF-β also induces activation of the MAPK pathways through upstream mediators Ras, RhoA, and TGF-β-activated kinase 1 (TAK1) (Yamaguchi *et al.*, 1995).

TGF-β was originally identified for its ability to transform normal rat kidney (NRK) fibroblasts *in vitro*, and this effect was required for the presence of EGF (Roberts *et al.*, 1981). FGF and TGF-β synergistically induce mesoderm in vertebrate development (Kimelman and Kirschner, 1987). Collectively, TGF-β can act synergistically with ligands signaling via receptor tyrosine kinases. Recent reports regarding R-Smads phosphorylation at linker regions upon HGF or EGF treatment (Kretzschmar *et al.*, 1997, 1999) have indicated that R-Smads proteins play a pivotal role in mediating crosstalk between receptor serine kinases and receptor tyrosine kinases. However, the molecular mechanisms and the biological implications of R-Smads phosphorylation via receptor serine kinases and receptor tyrosine kinases remain controversial (Kretzschmar *et al.*, 1997, 1999; de Caestecker *et al.*, 1998).

Without the antibodies (Abs) to selectively distinguish the phosphorylation sites of R-Smads, it has been difficult to determine the phosphorylation sites in intact cells and tissues. Therefore, we developed four types of polyclonal Abs, which specifically recognized the phosphorylated linker regions and the phosphorylated C-terminal SSXS regions in R-Smads (Furukawa *et al.*, 2003; Matsuzaki *et al.*, unpublished data). Using these phosphorylated domain-specific Abs, we examined whether HGF and TGF-β signals exerted an influence on R-Smads phosphorylation. Thereby, we tried to elucidate if R-Smads could mediate positive responses from both receptor serine kinases and receptor tyrosine kinases. In this paper, we showed that HGF as well as TGF-β could simultaneously stimulate the phosphorylation of endogenous R-Smads at their linker regions. The phosphorylation resulted in an enhanced hetero-oligomerization of R-Smads with Smad4 and nuclear translocation of the complex. JNK pathway involved HGF and TGF-β-mediated infiltration potency, which was caused partly by plasminogen activator inhibitor type 1 (PAI-1) induced via Smad3 phosphorylation at the linker region. These findings suggest that R-Smads phosphorylation at linker regions plays an important role in transmitting signals from receptor serine kinases and receptor tyrosine kinases.

Results

TGF-β signal simultaneously phosphorylates endogenous R-Smads not only at C-terminal regions but also at linker regions

Considerable amount of evidence supports the hypothesis that serine/threonine phosphorylation of R-Smads is involved in the Smad-mediated signal transduction. R-Smads possess two major phosphorylation sites: the linker region and the C-terminal region (Massagué, 1998). Phosphorylation of R-Smad takes place on the C-terminal two serine residues within the SSXS motif (Macías-Silva *et al.*, 1996). Accordingly, we generated a polyclonal Ab to the phosphorylated C-terminal region of Smad2 (α pSmad2C [Ser 465/467]) (Matsuzaki *et al.*, unpublished data), and that to the phosphorylated C-terminal region of Smad3 (α pSmad3C [Ser 423/425]) (Figure 1a) (Furukawa *et al.*, 2003). However, it was difficult to identify precise phoshorylation sites in their linker regions, because the linker regions possess four consensus phosphoacceptor sites for MAPK family members. Each linker region of Smad2 and Smad3 contains one consensus site for ERK (P*X*(S/T)P) (Davis, 1993; Hill and Treisman, 1995; Kretzschmar *et al.*, 1999) at Thr^{219} and at Thr^{178}, respectively. ERK-mediated phosphorylation of these sites has been shown to inhibit nuclear translocation of R-Smads and Smad-dependent transcription (Kretzschmar *et al.*, 1997, 1999). Besides the ERK phosphorylation sites, Smad2 and Smad3 contain a cluster of putative, non-ERK MAPK sites (*XX*(S/T)P) (Davis, 1993; Hill and Treisman, 1995) at $Ser^{244/249/254}$ and at $Ser^{203/207}$, respectively. On the other hand, the JNK pathway has been shown to have positive effects on Smad function (Brown *et al.*, 1999; Engel *et al.*, 1999). In addition, the linker sequence around $Ser^{249/254}$ in Smad2 is different from that around $Ser^{207/212}$ in Smad3. Therefore, we prepared phosphospecific polyclonal Abs designated α pSmad2L (Ser 249/254) (Matsuzaki *et al.*, unpublished data), and α pSmad3L (Ser 207/212) (Furukawa *et al.*, 2003), which selectively distinguish phosphorylation of Smad2 at the linker region from that of Smad3.

Initially, we investigated the time course of R-Smads phosphorylation in response to TGF-β stimulation. The serum-starved RGM-1 cells, which were isolated from normal rat gastric epithelial cells (Kobayashi *et al.*, 1996), were treated with TGF-β for various time intervals. R-Smads immunopurified with anti-R-Smads Ab were immunoblotted with each anti-phospho-R-Smad Ab (Figure 1b). Before stimulation, the linker sites of R-Smads were slightly phosphorylated under the basal conditions. In contrast, the phosphorylation level was insignificant at the C-terminal regions of R-Smads. TGF-β-dependent-phosphorylation occurred on two serine residues within the linker regions as well as within the C-terminal regions. R-Smads phosphorylation at linker regions and those at the C-terminal regions were detected within 5 min after TGF-β treatment, reached a maximum at 30 min, and decreased thereafter. However, Smad3 phosphorylation at the linker region was persistently observed after 2 h of TGF-β treatment. These results suggest that TGF-β signal simultaneously phosphorylates endogenous R-Smads not only at C-terminal regions but also at linker regions.

HGF signal phosphorylates endogenous R-Smads at linker regions but not at C-terminal regions

We further investigated whether endogenous R-Smads were phosphorylated in response to HGF. In contrast to

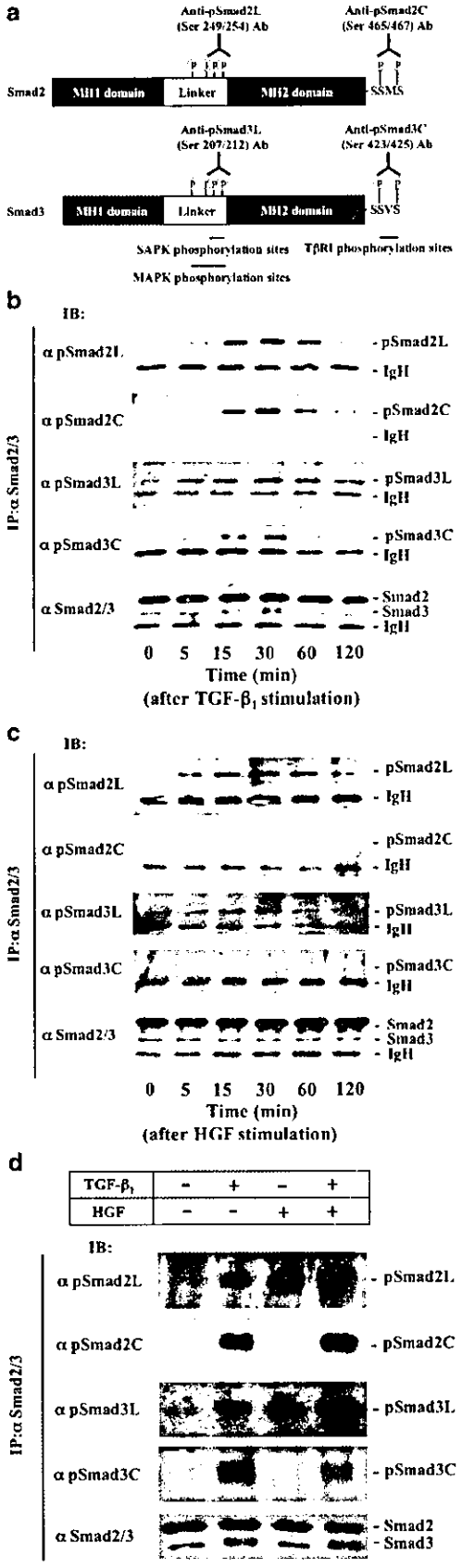

R-Smads phosphorylation at linker regions as well as C-terminal regions upon TGF-β treatment, HGF-dependent phosphorylation occurred on two serine residues within the linker regions but not within the C-terminal regions (Figure 1c). R-Smads phosphorylation at linker regions was detected within 5 min after HGF treatment, reached a maximum at 30 min, and decreased thereafter. These results suggest that HGF-mediated signal induces selective phosphorylation of endogenous R-Smads at linker regions.

TGF-β and HGF signals additionally phosphorylate the linker regions of R-Smads

We further investigated whether HGF treatment could affect R-Smads phosphorylation in response to TGF-β at 30 min after simultaneous treatment with TGF-β and HGF (Figure 1d). Smad2 phosphorylation at the linker region was more sensitive to HGF than to TGF-β, whereas the effect of TGF-β on Smad3 phosphorylation at the linker region was almost equal to that observed with HGF. R-Smads phosphorylation at linker regions was additionally stimulated by both TGF-β and HGF treatment. Taken together, these results suggest that common molecules activated by TGF-β and HGF signals might phosphorylate the linker regions of R-Smads. As already mentioned, TGF-β but not HGF treatment strongly enhanced R-Smads phosphorylation at the C-terminal regions. Smad2 phosphorylation at

Figure 1 HGF as well as TGF-β treatment induces endogenous R-Smads phosphorylation at linker regions, whereas the phosphorylation at their C-terminal regions were not induced by HGF treatment. (**a**) Antibodies selectively distinguish R-Smads phosphorylation at linker regions and at C-terminal SSXS regions. Anti-pSmad2L (Ser 249/254) Ab and anti-pSmad3L (Ser 207/212) Ab recognize SAPK phosphorylation sites in R-Smads, whereas anti-pSmad2C (Ser 465/467) Ab and anti-pSmad3C (Ser 423/425) Ab recognize the phosphorylated C-terminal SSXS sites in R-Smads that TβRI activates. (**b**) TGF-β signal simultaneously phosphorylates endogenous R-Smads not only at C-terminal regions but also at linker regions. RGM-1 cells were starved for 15 h in serum-free medium, and were incubated with 200 pM TGF-β for the indicated times. Following immunoprecipitation (IP) of the cell lysates with anti-Smad2/3 Ab, the phosphorylation levels of R-Smads were analysed by immunoblot (IB) using each anti-phospho-R-Smad Ab. The expression of endogenous Smad2 and Smad3 was monitored by immunoblot using anti-Smad2/3 Ab (lower panel). (**c**) HGF signal phosphorylates endogenous R-Smads at linker regions but not at C-terminal regions. RGM-1 cells were starved for 15 h in serum-free medium, and were incubated with 400 pM HGF for the indicated times. Following immunoprecipitation (IP) of the cell lysates with anti-Smad2/3 Ab, the phosphorylation levels of R-Smads were analysed by immunoblot (IB) using each anti-phospho-R-Smad Ab. The expression of endogenous Smad2 and Smad3 was monitored by immunoblot using anti-Smad2/3 Ab (lower panel). (**d**) TGF-β and HGF signals additionally phosphorylate the linker regions of R-Smads. RGM-1 cells were starved for 15 h in serum-free medium, and were incubated for 30 min with 200 pM TGF-β, 400 pM HGF, or a combination of both. Following immunoprecipitation (IP) of the cell lysates with anti-Smad2/3 Ab, the phosphorylation levels of R-Smads were analysed by immunoblot (IB) using each anti-phospho-R-Smad Ab. The expression of endogenous Smad2 and Smad3 was monitored by immunoblot using anti-Smad2/3 Ab (lower panel)

the C-terminal region was increased by simultaneous treatment with TGF-β and HGF. In contrast, both TGF-β and HGF treatment did not so much induce Smad3 phosphorylation at the C-terminal region as TGF-β treatment alone.

Collaborative interaction of TGF-β and HGF signals in JNK phosphorylation

MAPK pathways were shown to be activated in response to TGF-β and HGF (Robinson and Cobb, 1997; Mulder, 2000). We next investigated the time course of JNK, p38 MAPK, and ERK activation in response to TGF-β stimulation. RGM-1 cells were starved for 15 h in serum-free medium, and were treated with TGF-β for the indicated times. The activities of MAPKs were monitored by immunoblot using the Abs specific to the phosphorylated JNK, p38 MAPK, and ERK (Figure 2a–c). JNK and ERK phosphorylation induced by TGF-β treatment was very rapidly; the phosphorylation peaked 5 min after TGF-β treatment, and declined to the basal level by 1 h. However, p38 MAPK phosphorylation was detected after 30 min, reached a maximum at 60 min, and remained elevated during 2 h of TGF-β treatment. Likewise, JNK and ERK phosphorylation induced by HGF treatment was very rapid (Figure 2d–f). In contrast to the delayed response to TGF-β, HGF rapidly activated p38 MAPK. The phosphorylation was detected within 5 min upon HGF treatment, reached a maximum within the first 15 min, and gradually declined thereafter. We next investigated whether HGF treatment could affect JNK phosphorylation in response to TGF-β (Figure 2g). At 15 min after simultaneous treatment with TGF-β and HGF, the JNK phosphorylation was additionally stimulated.

JNK additionally activated by TGF-β and HGF signals directly phosphorylates R-Smads at linker regions

Because TGF-β and HGF signals phosphorylated JNK (Figure 2a, d) and thereafter R-Smads at linker regions (Figure 1b, c), we next investigated whether endogenous JNK activated by TGF-β and HGF signals could directly phosphorylate R-Smads *in vitro*. For this, we performed *in vitro* kinase assay, which is the most reliable method for studying the TGF-β-activated MAPKs. The serum-starved RGM-1 cells were extracted at 15 min after TGF-β and/or HGF treatment when the JNK phosphorylation reached a maximum (Figure 2a, d). Immunoprecipitate of the cell extract with the Ab against phospho-JNK was mixed with bacterially expressed GST-Smad2 and GST-Smad3. The phosphorylation levels of R-Smads were monitored by immunoblot using anti-phospho-Smad2L and -Smad3L Abs. JNK additionally activated by both TGF-β and HGF signals could directly phosphorylate Smad2 and Smad3 at linker regions *in vitro* (Figure 3a, b, upper panels). However, JNK failed to phosphorylate Smad2 and Smad3 at C-terminal regions upon TGF-β or HGF treatment (data not shown). Collectively, these data indicate that both Smad2 and Smad3 serve as the substrates for JNK *in vitro* after TGF-β and HGF treatment. In comparison with JNK, p38 MAPK activated at 15 min after HGF treatment failed to phosphorylate Smad2 at the linker region, but it could phosphorylate Smad3 at the linker region (data not shown). As a control, ERK activated by TGF-β signal could not phosphorylate Smad2 and Smad3 at these sites; moreover, a MEK1 inhibitor PD98059 treatment had no effect on the phosphorylation (data not shown).

Both JNK and p38 MAPK involve Smad3 phosphorylation at the linker region

To confirm the involvement of JNK and p38 MAPK in R-Smads phosphorylation *in vivo*, RGM-1 cells were preincubated with a JNK inhibitor SP600125 or a p38 MAPK inhibitor PD169316, and then the cells were stimulated with TGF-β and/or HGF for 30 min. SP600125 selectively inhibited TGF-β or HGF-mediated R-Smads phosphorylation at linker regions, but failed to inhibit the phosphorylation at C-terminal regions (Figures 1d and 4a). When R-Smads phosphorylation at linker regions was inhibited by SP600125, HGF treatment did not affect R-Smads phosphorylation at C-terminal regions regulated by TGF-β. In contrast, PD169316 partially inhibited not TGF-β but HGF-dependent Smad3 phosphorylation at the linker region (Figures 1d and 4b). When HGF-dependent Smad3 phosphorylation at the linker region was inhibited by PD169316, HGF treatment could not so much reduce Smad3 phosphorylation at the C-terminal region stimulated by TGF-β. Neither TGF-β nor HGF-mediated Smad2 phosphorylation at the linker region was inhibited by PD169316. These results were consistent with the findings that both Smad2 and Smad3 could serve as the substrates for JNK *in vitro* following TGF-β treatment (Figure 3), whereas the activated p38 MAPK could directly phosphorylate not Smad2 but Smad3 at the linker region *in vitro* (data not shown). In contrast to rapid response to HGF, p38 MAPK phosphorylation induced by TGF-β treatment was slow and persistent; p38 MAPK phosphorylation reached a maximum at 60 min, and remained elevated during 2 h of TGF-β treatment (Figure 2b, e). Collectively, Smad3 phosphorylation at the linker region at 30 min after TGF-β treatment could be mainly caused by the activated JNK, whereas p38 MAPK might persistently phosphorylate Smad3 at the linker region in RGM-1 cells (Figure 1b).

JNK-dependent R-Smads phosphorylation at linker regions induced by either TGF-β or HGF treatment allows R-Smads to associate with Smad4

R-Smads/Smad4 complexes translocate into the nucleus, where they activate the TGF-β-responsive genes. Accordingly, we investigated whether HGF signal had an effect on the complex formation. After RGM-1 cells were treated with TGF-β and/or HGF, the cell lysates were immunoprecipitated with each

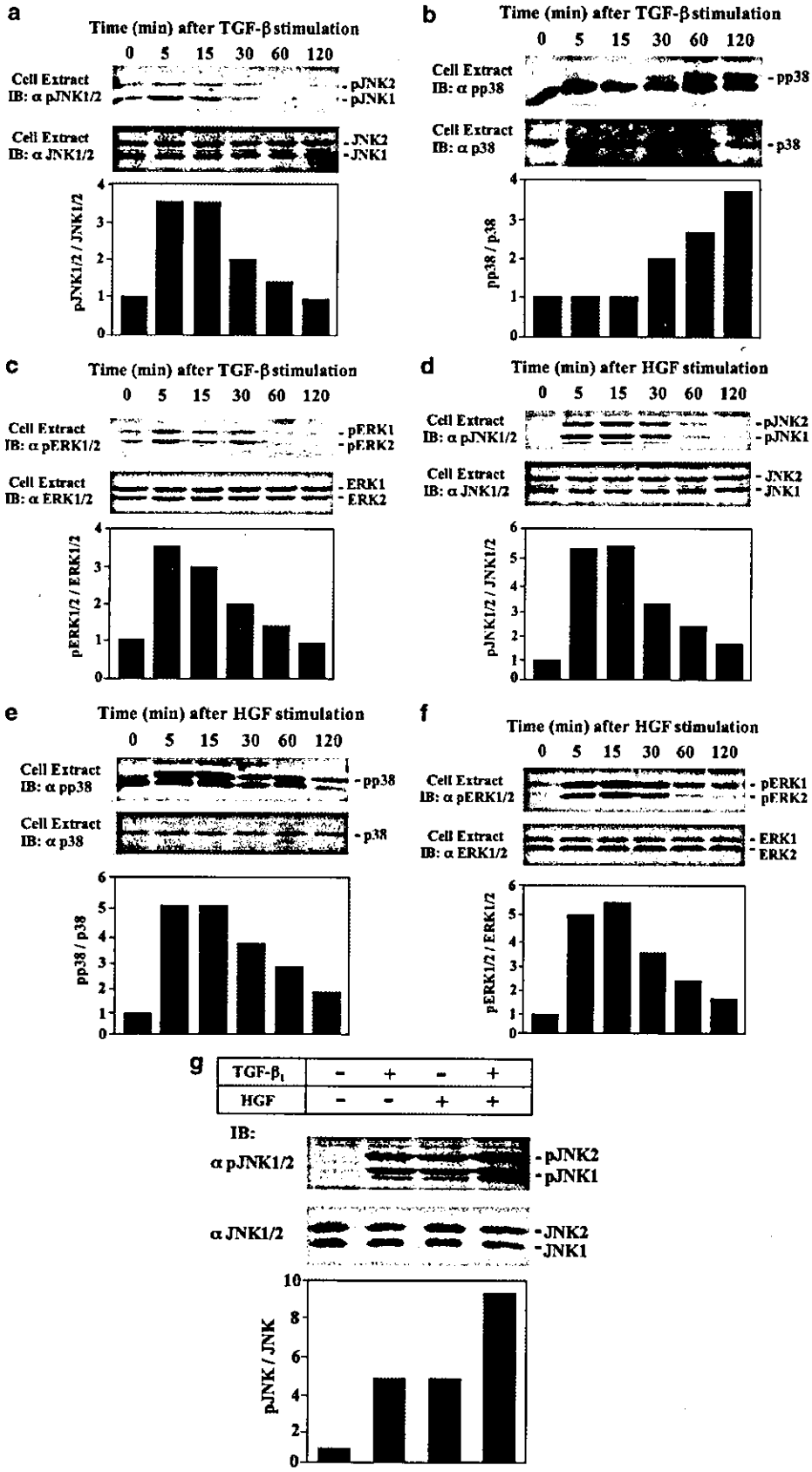
a
Time (min) after TGF-β stimulation
0 5 15 30 60 120
Cell Extract IB: α pJNK1/2
- pJNK2
- pJNK1
Cell Extract IB: α JNK1/2
- JNK2
- JNK1
pJNK1/2 / JNK1/2
b
Time (min) after TGF-β stimulation
0 5 15 30 60 120
Cell Extract IB: α pp38
- pp38
Cell Extract IB: α p38
- p38
pp38 / p38
c
Time (min) after TGF-β stimulation
0 5 15 30 60 120
Cell Extract IB: α pERK1/2
- pERK1
- pERK2
Cell Extract IB: α ERK1/2
- ERK1
- ERK2
pERK1/2 / ERK1/2
d
Time (min) after HGF stimulation
0 5 15 30 60 120
Cell Extract IB: α pJNK1/2
- pJNK2
- pJNK1
Cell Extract IB: α JNK1/2
- JNK2
- JNK1
pJNK1/2 / JNK1/2
e
Time (min) after HGF stimulation
0 5 15 30 60 120
Cell Extract IB: α pp38
- pp38
Cell Extract IB: α p38
- p38
pp38 / p38
f
Time (min) after HGF stimulation
0 5 15 30 60 120
Cell Extract IB: α pERK1/2
- pERK1
- pERK2
Cell Extract IB: α ERK1/2
- ERK1
- ERK2
pERK1/2 / ERK1/2
g
TGF-β1 - + - +
HGF - - + +
IB:
α pJNK1/2
- pJNK2
- pJNK1
α JNK1/2
- JNK2
- JNK1
pJNK / JNK

anti-phospho-R-Smad Ab, and Smad4 in the immunoprecipitate was detected by immunoblot using anti-Smad4 Ab. As shown in Figure 5a, interactions between the phosphorylated R-Smads and Smad4 were scarcely present in the unstimulated culture. TGF-β treatment induced the complex formation of the phosphorylated R-Smads with Smad4. Similarly, treatment of the cells with HGF induced the complex formation between R-Smads phosphorylated at linker regions and Smad4. However, increase in the associations between R-Smads phosphorylated at the C-terminal regions and Smad4 was not observed in the cells treated with HGF. These results, coupled with the findings shown in Figures 1c and 3, suggest that HGF-mediated association of R-Smads with Smad4 is JNK-dependent. Additional treatment of HGF with TGF-β led to an increase in the association between Smad2 phosphorylated at the linker region and Smad4. Similarly, both TGF-β and HGF treatment increased the association between Smad2 phosphorylated at the C-terminal region and Smad4. These data indicate that TGF-β and HGF additionally induce the complex formation of Smad2 with Smad4 through Smad2 phosphorylation both at the linker region and at the C-terminal region. In contrast, additional treatment of HGF with TGF-β did not so much stimulate the associations between the phosphorylated Smad3 and Smad4 as TGF-β treatment alone. Difficulty of these associations between Smad3 and Smad4 might be due to higher affinity of Smad4 to the phosphorylated Smad2 than those to Smad3.

We further investigated effects of SP600125 on the complex formation of phosphorylated R-Smads with Smad4 (Figure 5b). RGM-1 cells were preincubated with SP600125, and then were stimulated with TGF-β and/or HGF. SP600125 selectively inhibited TGF-β or HGF-mediated complex formation between R-Smads phosphorylated at linker regions and Smad4, but failed to inhibit the complex formation between R-Smads phosphorylated at C-terminal regions and Smad4. When R-Smads phosphorylation at linker regions was inhibited by SP600125, HGF treatment did not affect TGF-β-mediated complex formation between R-Smads phosphorylated at C-terminal regions and Smad4.

Consistent with the observation that HGF-mediated signal induces phosphorylation of endogenous R-Smads at linker regions but not at C-terminal regions (Figure 1c), HGF-dependent R-Smads phosphorylation at linker regions was observed in R-Smads(3S-A) lacking C-terminal serine residues, but not in R-Smads EPSM lacking phosphorylation sites in the linker regions (data not shown). We therefore decided to investigate whether HGF-dependent signaling occurred at the downstream steps in these R-Smads mutants. RGM-1 cells were transfected with Smad4-HA in the presence of Flag-Smad2WT, Smad2EPSM, or Smad2(3S-A). The cell lysates were immunoprecipitated with anti-Flag Ab, and Smad4 in the immunoprecipitate was detected by immunoblot using anti-HA Ab. As shown in Figure 5c, marginal interaction between Smad2 and Smad4 was observed in the unstimulated culture. A significant increase in the association of Smad2WT with Smad4 was observed in the cells after HGF treatment. HGF treatment induced relatively weak interactions between Smad2(3S-A) and Smad4, as compared with HGF-dependent interaction of Smad2WT with Smad4. However, HGF treatment failed to increase the interaction of Smad2EPSM with Smad4. The ligand-dependent interaction of the activated Smad3 with Smad4 was observed similarly in Smad3(3S-A) but not in Smad3EPSM (Figure 5d). These results, coupled with the findings shown in Figure 1c, suggest that HGF treatment induces the association of R-Smads with Smad4 through the linker phosphorylation, but not through the C-terminal phosphorylation.

Simultaneous treatment with HGF and TGF-β leads to stimulate nuclear translocation of R-Smads phosphorylated at linker regions

Translocation of R-Smads into the nucleus upon receptor-mediated phosphorylation is a central event in TGF-β signal transduction (Macías-Silva *et al.*, 1996). To gain additional insight into the significance of R-Smads phosphorylation, we examined intracellular localization of the phospho-R-Smads. To this end, we treated RGM-1 cells with TGF-β and/or HGF, and observed intracellular localization by indirect immunofluorescence microscopy using each anti-phospho-R-Smad Ab (Figure 6a). R-Smads were scarcely phosphorylated in the absence of exogenous TGF-β. In all, 85% Smad2 phosphorylated at the linker region was located in cytoplasm upon TGF-β or HGF treatment, whereas additional treatment of HGF with TGF-β

Figure 2 Collaborative interaction of TGF-β and HGF signals in JNK phosphorylation. RGM-1 cells were starved for 15 h in serum-free medium, and were incubated with 200 pM TGF-β (**a, b, c**) or 400 pM HGF (**d, e, f**) for the indicated times. The phosphorylation levels of endogenous MAPKs were analysed by immunoblot (IB) using anti-phospho-JNK1/2 Ab (α pJNK1/2) (**a, d**), anti-phospho-p38 MAPK Ab (α pp38) (**b, e**), and anti-phospho-ERK1/2 Ab (α pERK1/2) (**c, f**). The total amount of each MAPK did not change during stimulation (lower panel). (**g**) TGF-β and HGF signals additionally stimulate JNK phosphorylation. Serum-starved RGM-1 cells were incubated for 15 min with 200 pM TGF-β, 400 pM HGF, or a combination of both. The phosphorylation levels of endogenous JNK1/2 were determined by immunoblot using anti-phospho-JNK1/2 Ab (α pJNK1/2) (upper panel). The expression of endogenous JNK1/2 was monitored by immunoblot using anti-JNK1/2 Ab (α JNK1/2) (lower panel). Bottom: Graphical analyses of immunoblots showing the ratio of phospho-JNK1/2 to total JNK1/2 (**a, d, g**), phospho-p38 to total p38 (**b, e**) or phospho-ERK1/2 to total ERK1/2 (**c, f**) after stimulation with TGF-β and/or HGF. Intensities of phospho-JNK1/2, p38 or ERK1/2 bands were normalized to those of total JNK1/2, p38 or ERK1/2 of the corresponding treatment groups. The ratio of the phosphorylated protein to total protein without exogenous TGF-β or HGF is assigned a value of 1

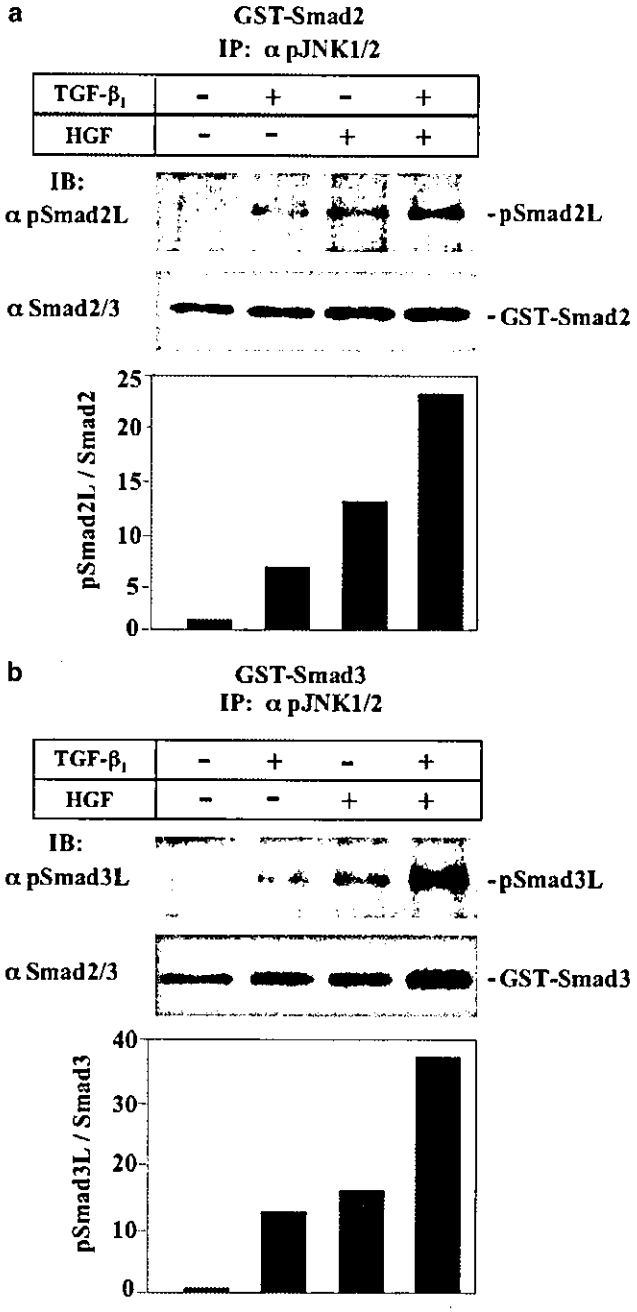

Figure 3 JNK activated by TGF-β and/or HGF signals directly phosphorylates R-Smads at linker regions. RGM-1 cells were starved for 15 h in serum-free medium, and were incubated for 15 min with 200 pM TGF-β, 400 pM HGF, or a combination of both. Cell extracts were immunoprecipitated with anti-phospho-JNK1/2 Ab. *In vitro* kinase assays were performed using GST-Smad2 (**a**) and GST-Smad3 (**b**) as substrates. The phosphorylated states of R-Smads were analysed by immunoblot (IB) using each anti-phospho-R-Smad Ab (upper panel). Total Smad2 and Smad3 were monitored by immunoblot (IB) using anti-Smad2/3 Ab (lower panel). Bottom: Graphical analyses of immunoblots showing the ratio of phospho-Smad2 to total Smad2 (**a**) or phospho-Smad3 to total Smad3 (**b**) after stimulation with TGF-β and/or HGF. Intensities of phospho-Smad2 or Smad3 bands were normalized to those of total Smad2 or Smad3 of the corresponding treatment groups. The ratio of the phosphorylated protein to total protein without exogenous TGF-β or HGF is assigned a value of 1

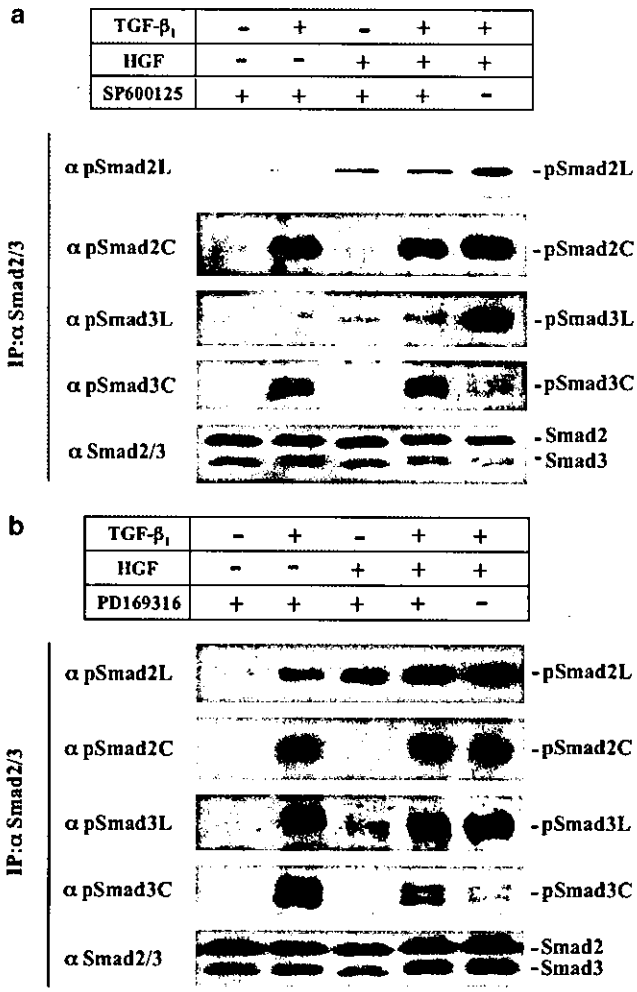

Figure 4 Both JNK and p38 MAPK involve Smad3 phosphorylation at the linker region. Serum-starved RGM-1 cells were incubated with 10 μM SP600125 (**a**) or 10 μM PD169316 (**b**) for 8 h, and then were stimulated with 200 pM TGF-β, 400 pM HGF, or a combination of both for 30 min. Following immunoprecipitation (IP) of the cell lysates with anti-Smad2/3 Ab, the phosphorylation levels of R-Smads were analysed by immunoblot (IB) using each anti-phospho-R-Smad Ab. The expression of endogenous R-Smads was monitored by immunoblot using anti-Smad2/3 Ab

translocated the phosphorylated Smad2 into the nuclei. Taken together with the results of a report that forced expression of a constitutively active form of mitogen-activated protein kinase kinase kinase-1 (MEKK-1), which is an upstream activator of the JNK pathway, stimulates nuclear localization of Smad2 (Brown *et al.*, 1999), these results indicate that Smad2 phosphorylated at the linker region sets a high threshold for nuclear translocation. Otherwise, Smad2 phosphorylated at the linker region might remain in the cytoplasm as far as TβRI-mediated Smad2 phosphorylation does not occur at the C-terminal site. In contrast, either TGF-β or HGF treatment alone led to nuclear translocation of Smad3 phosphorylated at the linker region, and both treatment additionally stimulated this nuclear translocation. Likewise, Smad3 phosphorylation by JNK facilitates its nuclear accumulation (Engel *et al.*, 1999).

These results indicate that Smad3 phosphorylated at the linker region has a lower threshold for nuclear translocation than does the phosphorylated Smad2. As expected, most Smad2 phosphorylated at the C-terminal region was located in the nuclei upon TGF-β treatment. In contrast, exposure to excess HGF did not lead to nuclear accumulation of the phosphorylated Smad2. Similarly, nuclear accumulation of Smad3 phosphorylated at the C-terminal region was stimulated by TGF-β treatment, but not by HGF treatment. Consistent with the reduced Smad3 phosphorylation at the C-terminal region (Figure 1d), additional treatment of HGF with TGF-β did not so much induce the nuclear accumulation of the phosphorylated Smad3 as TGF-β treatment alone. These results could be explained by inaccessibility of Smad3 to TβRI as a result of JNK-dependent nuclear localization of Smad3.

We further investigated the effects of SP600125 on intracellular localization of phosphorylated R-Smads (Figure 6b). RGM-1 cells were preincubated with SP600125, and then were stimulated with TGF-β and/or HGF. SP600125 selectively inhibited TGF-β or HGF-mediated intracellular localization of R-Smads phosphorylated at linker regions, but failed to inhibit nuclear localization of R-Smads phosphorylated at C-terminal regions.

SP600125 treatment causes the reduction of invasive capacity induced by TGF-β and HGF signals

Both HGF and TGF-β are proposed as main participants in the promotion of tumor cell invasion and metastasis (Stoker *et al*., 1987; Wakefield and Roberts, 2002). We therefore investigated whether HGF and TGF-β enhanced infiltration potency of RGM-1 cells,

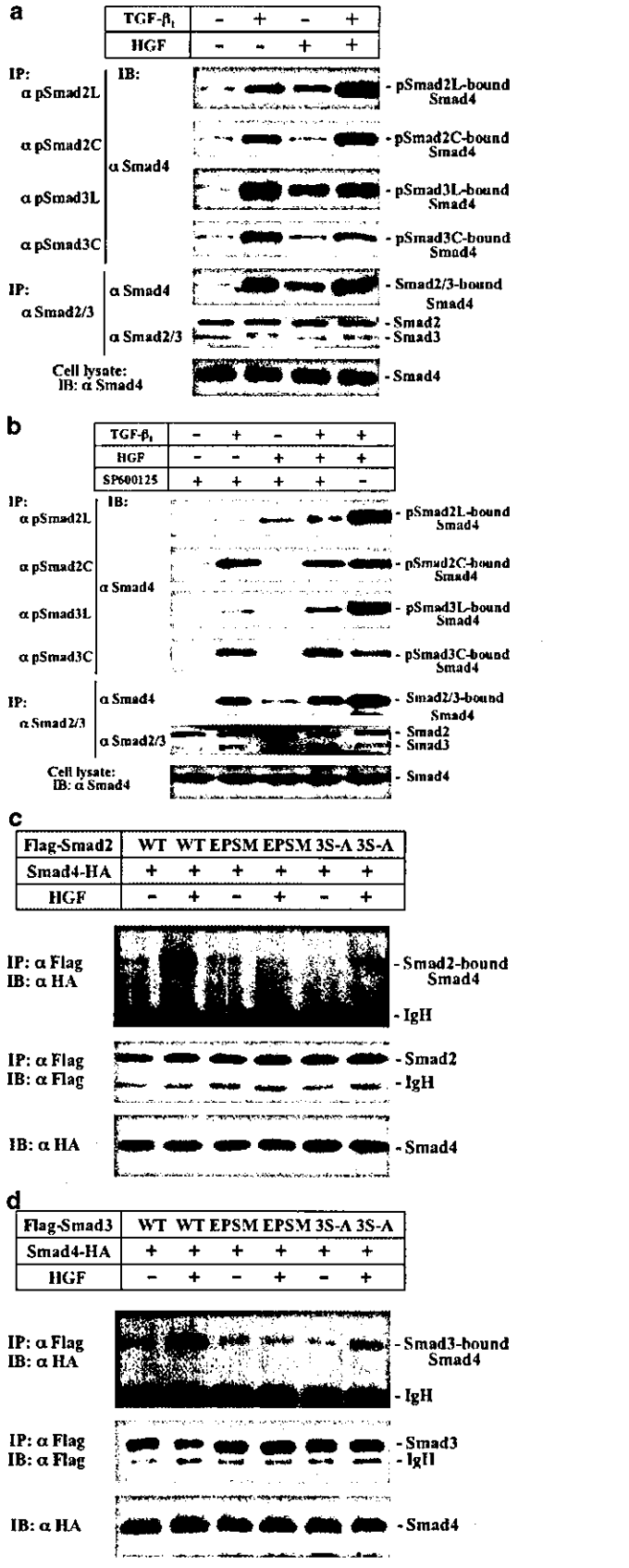

Figure 5 JNK-dependent R-Smads phosphorylation at linker regions induced by either TGF-β or HGF treatment allows R-Smads to associate with Smad4. Serum-starved RGM-1 cells were incubated for 8 h in the absence (**a**) or presence (**b**) of 10 μM SP600125, and were then treated for 40 min with 200 pM TGF-β, 400 pM HGF, or a combination of both. Cell lysates were subjected to immunoprecipitation (IP) with each anti-phospho-R-Smad Ab or anti-R-Smads Ab, and Smad4 in the immunoprecipitate was detected by immunoblot (IB) using anti-Smad4 Ab. Total Smad4 and Smad2/3 were monitored by immunoblot (IB) using anti-Smad4 Ab and anti-Smad2/3 Ab, respectively (lower panels). (**c**) HGF treatment induces the complex formation of Smad2(3S-A) with Smad4. RGM-1 cells were transfected with Smad4-HA in the presence of Flag-Smad2WT, Smad2EPSM, or Smad2(3S-A), and were treated with HGF. The cell lysates were then subjected to immunoprecipitation (IP) with anti-Flag Ab, and Smad4 in the immunoprecipitate was detected by immunoblot (IB) using anti-HA Ab. The expression of Flag-Smad2 and Smad4-HA was monitored by immunoblot (IB) using anti-Flag Ab and anti-HA Ab, respectively. (**d**) HGF treatment induces the complex formation of Smad3(3S-A) with Smad4. RGM-1 cells were transfected with Smad4-HA in the presence of Flag-Smad3WT, Smad3EPSM, or Smad3(3S-A), and were treated with HGF. The cell lysates were then subjected to immunoprecipitation (IP) with anti-Flag Ab, and Smad4 in the immunoprecipitate was detected by immunoblot (IB) using anti-HA Ab. The expression of Flag-Smad3 and Smad4-HA was monitored by immunoblot (IB) using anti-Flag Ab and anti-HA Ab, respectively

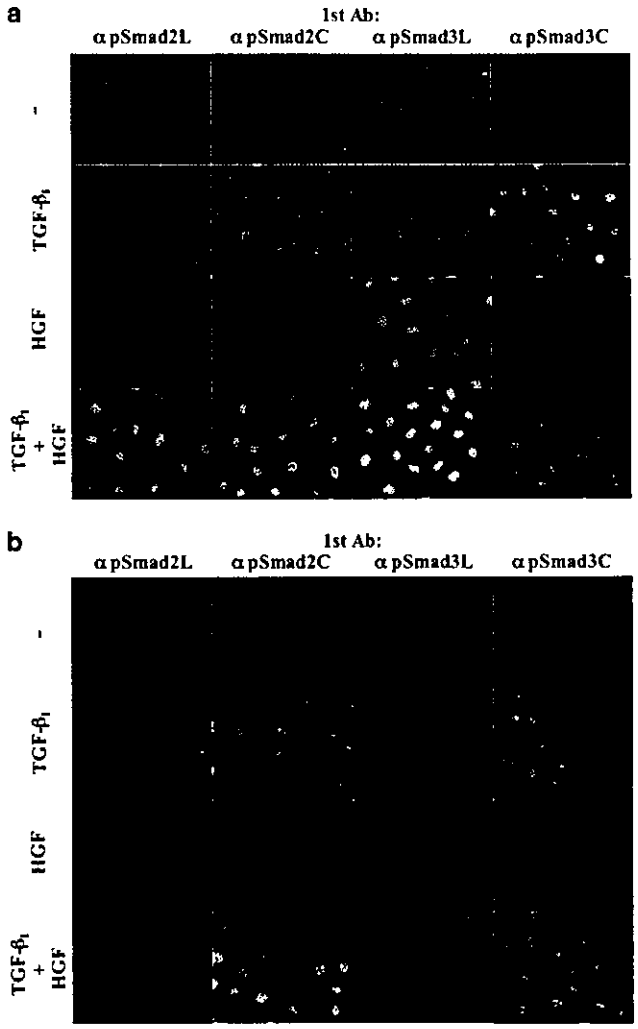

Figure 6 Simultaneous treatment with TGF-β and HGF leads to stimulate nuclear translocation of R-Smads phosphorylated at linker regions. Serum-starved RGM-1 cells were incubated for 8 h in the absence (**a**) or presence (**b**) of 10 μM SP600125. The cells were then treated for 60 min with 200 pM TGF-β, 400 pM HGF, or a combination of both. After fixation with 4% paraformaldehyde, the slides were incubated with a primary Ab at 4°C for 16 h. Localization of the phosphorylated R-Smads was visualized by each anti-phospho-R-Smad immunofluorescence

and SP600125 had any effects on HGF and/or TGF-β-mediated infiltration potency. RGM-1 cells were cultured on Matrigel for 48 h with TGF-β and/or HGF in the presence or absence of a JNK inhibitor SP600125 (Figure 7). No cytotoxicity was observed at the concentrations of SP600125 tested in these assays. When RGM-1 cells were not stimulated, most cells remained in the upper chamber. Either TGF-β or HGF treatment led to increase in the infiltration potency of RGM-1 cells. Additional treatment of HGF with TGF-β increased the infiltration potency above that of TGF-β or HGF treatment alone. On the other hand, SP600125 showed the suppressive effects on the infiltrating potency triggered by TGF-β and/or HGF stimulation, suggesting that JNK pathway involved TGF-β and/or HGF-mediated infiltration potency.

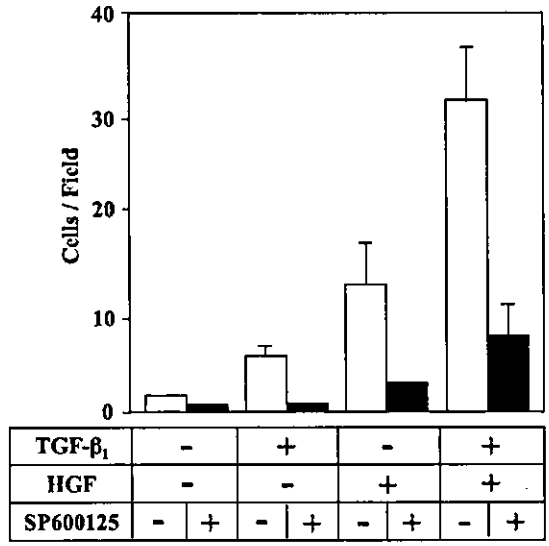

Figure 7 JNK inhibitor SP600125 treatment causes the reduction of invasive capacity induced by TGF-β and HGF signals. RGM-1 cells were cultured on Matrigel for 48 h with 200 pM TGF-β_1 and/or 400 pM HGF in the absence or presence of 10 μM SP600125. After fixation with 100% methanol, the cells were stained by hematoxylin. The number of infiltrating cells were counted in five regions selected at random, and the extent of invading cells was determined by the mean count. Duplicate filters were used, and the experiments were repeated three times

TGF-β and HGF signals stimulate PAI-1 transcription through Smad3 phosphorylation at the linker region

The processes of cellular invasion are characterized, in part, by altered local proteolysis and stimulating cell growth. Plasminogen activator inhibitor type 1 (PAI-1), the main inhibitor of the urokinase-type plasminogen activator system, conducts the cells to migration and invasion by blocking cellular adhesion and by promoting basement membrane degradation (Gutierrez *et al.*, 2000). Moreover, PAI-1-induced TGF-β signal stimulates attachment and invasion in primary ovarian cancer cells (Hirashima *et al.*, 2003). Therefore, we investigated whether HGF and TGF-β regulated PAI-1 expression in RGM-1 cells. Northern blot analyses of *PAI-1* on RNA prepared from RGM-1 cells revealed that *PAI-1* mRNA (3.2 kb) were rapidly induced either by TGF-β or HGF (Figure 8a). Additional treatment of HGF with TGF-β enhanced PAI-1 upregulation at the mRNA level, when compared with those upon HGF or TGF-β treatment alone.

To investigate the role of JNK in the regulation of TGF-β and HGF signaling, we next examined effects of dominant-negative form of MEKK-1 on the activities of PAI-1 promoter. For the assays, we used PF1-Luc, because the segment in human PAI-1 promoter was sufficient to obtain TGF-β-dependent induction (Hua *et al.*, 1998). RGM-1 cells transfected PF1-Luc alone showed a low level of transcriptional activity (Figure 8b). TGF-β strongly induced the transcriptional activity, and HGF treatment led to an increase in the transcriptional

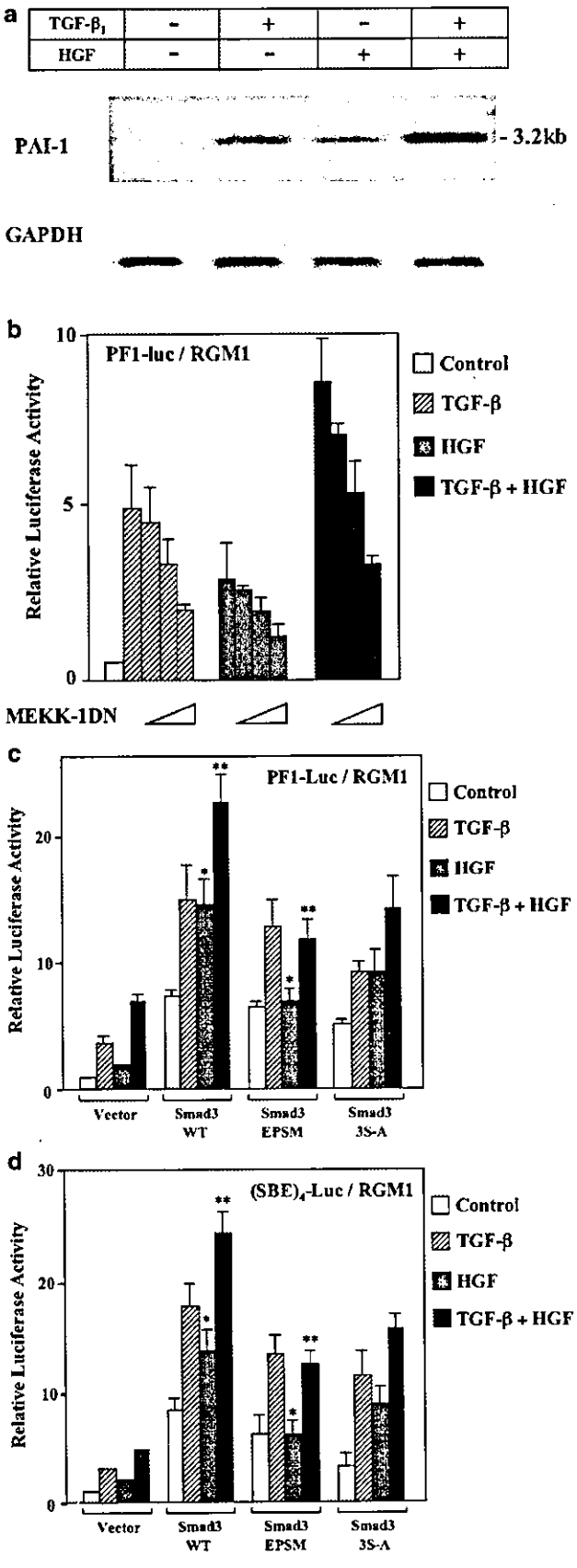

activity. Additional treatment of HGF with TGF-β increased the transcriptional activity above that of TGF-β treatment alone. In addition, the transcriptional induction by either TGF-β or HGF was partially inhibited by the dominant-negative form of MEKK-1. Similarly, the induction by additional treatment of HGF with TGF-β was inhibited by dominant-negative form of MEKK-1. Taken together, these results suggest that transcriptional induction of PAI-1 promoter by TGF-β and HGF requires the action of MEKK-1.

Fibroblast derived from mouse embryos deficient in Smad3 showed that TGF-β-mediated induction of PAI-1 transcript was mainly dependent on Smad3 (Piek *et al*., 2001). To determine whether HGF and TGF-β transmit their signals through Smad3 phosphorylation at the linker region, we further investigated the effect of this phosphorylation on PAI-1 transcription. In cells cotransfected of PF1-Luc with Smad3WT, treatment with TGF-β induced an increase in the transcriptional activity (Figure 8c). HGF treatment alone similarly activated the transcription. Moreover, additional treatment of HGF with TGF-β led to an increase in the transcriptional activity, when compared with that upon TGF-β treatment alone. Cotransfection with Smad3EPSM, which lacked phosphorylation sites in the linker region, induced an increase of the transcriptional activity triggered by TGF-β stimulation, whereas it could not significantly modify the transcriptional activity in RGM-1 cells treated with HGF alone. Similarly, a combined treatment with TGF-β and HGF of the cells expressing Smad3EPSM did not lead to an additional increase in the transcriptional activity. Cotransfection with Smad3(3S-A) as a control, which lacked C-terminal serine residues, induced an increase of the transcriptional activities triggered by either TGF-β or

Figure 8 TGF-β and HGF signals additionally stimulate PAI-1 transcriptional activity through Smad3 phosphorylation at the linker region. (**a**) TGF-β and HGF upregulate PAI-1 expression at the mRNA level. Northern blot hybridization was performed with poly(A)$^+$ RNAs (2 μg/lane) from RGM-1 cells treated for 3 h with 200 pM TGF-β and/or 400 pM HGF. Blots were hybridized with ^{32}P-labeled random-primed cDNAs for PAI-1 (upper panel) and GAPDH (lower panel) as an internal control. (**b**) Transcriptional induction of PF1 promoter by TGF-β and HGF requires the action of MEKK-1. RGM-1 cells were transiently cotransfected of PF1-Luc with increasing amounts (1:1, 1:2.5, 1:5) of dominant-negative form of MEKK-1 (MEKK-1DN), and the cells were incubated for 4 h. After changing the medium, the cells were incubated for a further 30 h. Under serum-free conditions, the cells were incubated for 12 h with 200 pM TGF-β, 400 pM HGF, or a combination of both. Luciferase activity was determined and normalized to transfection efficiency. Values of samples from cells transfected with PF1-Luc alone and left untreated were arbitrarily set to 1. The results are the mean ± s.d. ($n=4$) from a representative experiment. (**c, d**) HGF signal stimulates transcriptional activities of PF1-Luc and $(SBE)_4$-Luc through Smad3 phosphorylation at the linker region. RGM-1 cells were transiently cotransfected of PF1-Luc (**c**) or $(SBE)_4$-Luc (**d**) with Smad3WT, Smad3EPSM, or Smad3(3S-A). Under serum-free conditions, the cells were incubated for 12 h with 200 pM TGF-β, 400 pM HGF, or a combination of both. Luciferase activities were determined above. *$P<0.05$, **$P<0.01$, by one-way analysis of variance